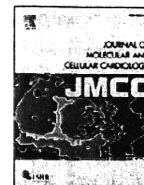


- Mammucari, C., Milan, G., Romanello, V., Masiero, E., Rudolf, R., Del Piccolo, P., Burden, S.J., Di Lisi, R., Sandri, C., Zhao, J., et al. (2007). FoxO3 controls autophagy in skeletal muscle in vivo. *Cell Metab.* 6, 458–471.
- Matthews, S.E. (1999). Proteins and amino acids. In *Modern Nutrition and Health and Diseases*, 9th ed., M.E. Shils, J.A. Olson, M. Shike, and A.C. Ross, eds. (Baltimore: Williams & Wilkins), pp. 11–48.
- Meijsing, S.H., Pufall, M.A., So, A.Y., Bates, D.L., Chen, L., and Yamamoto, K.R. (2009). DNA binding site sequence directs glucocorticoid receptor structure and activity. *Science* 324, 407–410.
- Menconi, M., Fareed, M., O'Neal, P., Poylin, V., Wei, W., and Hasselgren, P.O. (2007). Role of glucocorticoids in the molecular regulation of muscle wasting. *Crit. Care Med.* 35, S602–S608.
- Mizushima, N., Levine, B., Cuervo, A.M., and Klionsky, D.J. (2008). Autophagy fights disease through cellular self-digestion. *Nature* 451, 1069–1075.
- Moresi, V., Williams, A.H., Meadows, E., Flynn, J.M., Potthoff, M.J., McAnally, J., Shelton, J.M., Backs, J., Klein, W.H., Richardson, J.A., et al. (2010). Myogenin and class II HDACs control neurogenic muscle atrophy by inducing E3 ubiquitin ligases. *Cell* 143, 35–45.
- Munck, A., Guyre, P.M., and Holbrook, N.J. (1984). Physiological functions of glucocorticoids in stress and their relation to pharmacological actions. *Endocr. Rev.* 5, 25–44.
- Newgard, C.B., An, J., Bain, J.R., Muehlbauer, M.J., Stevens, R.D., Lien, L.F., Haqq, A.M., Shah, S.H., Arlotto, M., Slentz, C.A., et al. (2009). A branched-chain amino acid-related metabolic signature that differentiates obese and lean humans and contributes to insulin resistance. *Cell Metab.* 9, 311–326.
- Ning, Y.M., and Sanchez, E.R. (1993). Potentiation of glucocorticoid receptor-mediated gene expression by the immunophilin ligands FK506 and rapamycin. *J. Biol. Chem.* 268, 6073–6076.
- Risson, V., Mazelin, L., Roceri, M., Sanchez, H., Moncollin, V., Corneloup, C., Richard-Bulteau, H., Vignaud, A., Baas, D., Defour, A., et al. (2009). Muscle inactivation of mTOR causes metabolic and dystrophin defects leading to severe myopathy. *J. Cell Biol.* 187, 859–874.
- Sancak, Y., Bar-Peled, L., Zoncu, R., Markhard, A.L., Nada, S., and Sabatini, D.M. (2010). Regulator-Rag complex targets mTORC1 to the lysosomal surface and is necessary for its activation by amino acids. *Cell* 141, 290–303.
- Sandri, M. (2008). Signaling in muscle atrophy and hypertrophy. *Physiology (Bethesda)* 23, 160–170.
- Sandri, M., Sandri, C., Gilbert, A., Skurk, C., Calabria, E., Picard, A., Walsh, K., Schiaffino, S., Lecker, S.H., and Goldberg, A.L. (2004). Foxo transcription factors induce the atrophy-related ubiquitin ligase atrogin-1 and cause skeletal muscle atrophy. *Cell* 117, 399–412.
- Schakman, O., Gilson, H., and Thissen, J.P. (2008). Mechanisms of glucocorticoid-induced myopathy. *J. Endocrinol.* 197, 1–10.
- Sengupta, S., Peterson, T.R., and Sabatini, D.M. (2010). Regulation of the mTOR complex 1 pathway by nutrients, growth factors, and stress. *Mol. Cell* 40, 310–322.
- She, P., Reid, T.M., Bronson, S.K., Vary, T.C., Hajnal, A., Lynch, C.J., and Hutson, S.M. (2007). Disruption of BCATm in mice leads to increased energy expenditure associated with the activation of a futile protein turnover cycle. *Cell Metab.* 6, 181–194.
- Stitt, T.N., Drujan, D., Clarke, B.A., Panaro, F., Timofeyeva, Y., Kline, W.O., Gonzalez, M., Yancopoulos, G.D., and Glass, D.J. (2004). The IGF-1/PI3K/Akt pathway prevents expression of muscle atrophy-induced ubiquitin ligases by inhibiting FOXO transcription factors. *Mol. Cell* 14, 395–403.
- Suzuki, N., Motohashi, N., Uezumi, A., Fukada, S., Yoshimura, T., Itoyama, Y., Aoki, M., Miyagoe-Suzuki, Y., and Takeda, S. (2007). NO production results in suspension-induced muscle atrophy through dislocation of neuronal NOS. *J. Clin. Invest.* 117, 2468–2476.
- Um, S.H., D'Alessio, D., and Thomas, G. (2006). Nutrient overload, insulin resistance, and ribosomal protein S6 kinase 1, S6K1. *Cell Metab.* 3, 393–402.
- Waddell, D.S., Baehr, L.M., van den Brandt, J., Johnsen, S.A., Reichardt, H.M., Furlow, J.D., and Bodine, S.C. (2008). The glucocorticoid receptor and FOXO1 synergistically activate the skeletal muscle atrophy-associated MuRF1 gene. *Am. J. Physiol. Endocrinol. Metab.* 295, E785–E797.
- Wagenmakers, A.J. (1998). Protein and amino acid metabolism in human muscle. *Adv. Exp. Med. Biol.* 441, 307–319.
- Wang, H., Kubica, N., Ellisen, L.W., Jefferson, L.S., and Kimball, S.R. (2006). Dexamethasone represses signaling through the mammalian target of rapamycin in muscle cells by enhancing expression of REDD1. *J. Biol. Chem.* 281, 39128–39134.
- Yan, H., Frost, P., Shi, Y., Hoang, B., Sharma, S., Fisher, M., Gera, J., and Lichtenstein, A. (2006a). Mechanism by which mammalian target of rapamycin inhibitors sensitize multiple myeloma cells to dexamethasone-induced apoptosis. *Cancer Res.* 66, 2305–2313.
- Yoshikawa, N., Nagasaki, M., Sano, M., Tokudome, S., Ueno, K., Shimizu, N., Imoto, S., Miyano, S., Suematsu, M., Fukuda, K., et al. (2009). Ligand-based gene expression profiling reveals novel roles of glucocorticoid receptor in cardiac metabolism. *Am. J. Physiol. Endocrinol. Metab.* 296, E1363–E1373.
- Yu, L., McPhee, C.K., Zheng, L., Mardones, G.A., Rong, Y., Peng, J., Mi, N., Zhao, Y., Liu, Z., Wan, F., et al. (2010). Termination of autophagy and reformation of lysosomes regulated by mTOR. *Nature* 465, 942–946.
- Zhao, J., Brault, J.J., Schild, A., Cao, P., Sandri, M., Schiaffino, S., Lecker, S.H., and Goldberg, A.L. (2007). FoxO3 coordinately activates protein degradation by the autophagic/lysosomal and proteasomal pathways in atrophying muscle cells. *Cell Metab.* 6, 472–483.



Original article

Impact of long-term caloric restriction on cardiac senescence: Caloric restriction ameliorates cardiac diastolic dysfunction associated with aging

Ken Shinmura^{a,*}, Kayoko Tamaki^a, Motoaki Sano^{b,c}, Mitsushige Murata^b, Hiroyuki Yamakawa^b, Hideyuki Ishida^d, Keiichi Fukuda^b^a Division of Geriatric Medicine, Department of Internal Medicine, Keio University School of Medicine, Tokyo, 160-8582, Japan^b Division of Cardiology, Department of Internal Medicine, Keio University School of Medicine, Tokyo, 160-8582, Japan^c Precursory Research for Embryonic Science and Technology (PRESTO), Japan Science and Technology Agency, Saitama, 332-0012, Japan^d Department of Physiology, Tokai University School of Medicine, Isehara, 259-1193, Japan

ARTICLE INFO

Article history:

Received 2 June 2010

Received in revised form 5 October 2010

Accepted 17 October 2010

Available online 23 October 2010

Keywords:

Aging

Autophagy

Calcium

Cardiac function

Nutrition

Sarcoplasmic reticulum

ABSTRACT

Approximately half of older patients with congestive heart failure have normal left ventricular (LV) systolic but abnormal LV diastolic function. In mammalian hearts, aging is associated with LV diastolic dysfunction. Caloric restriction (CR) is expected to retard cellular senescence and to attenuate the physiological decline in organ function. Therefore, the aim of the present study was to investigate the impact of long-term CR on cardiac senescence, in particular the effect of CR on LV diastolic dysfunction associated with aging. Male 8-month-old Fischer344 rats were divided into ad libitum fed and CR (40% energy reduction) groups. LV function was evaluated by echocardiography and cardiac senescence was compared between the two groups at the age of 30-month-old. (1) Echocardiography showed similar LV systolic function, but better LV diastolic function in the CR group. (2) Histological analysis revealed that CR attenuated the accumulation of senescence-associated β -galactosidase and lipofuscin and reduced myocyte apoptosis. (3) In measurements of $[Ca^{2+}]_i$ transients, the time to 50% relaxation was significantly smaller in the CR group, whereas F/F_0 was similar. (4) CR attenuated the decrease in sarcoplasmic reticulum calcium ATPase 2 protein with aging. (5) CR suppressed the mammalian target of rapamycin (mTOR) pathway and increased the ratio of conjugated to cytosolic light chain 3, suggesting that autophagy is enhanced in the CR hearts. In conclusion, CR improves diastolic function in the senescent myocardium by amelioration of the age-associated deterioration in intracellular Ca^{2+} handling. Enhanced autophagy via the suppression of mTOR during CR may retard cardiac senescence.

© 2010 Elsevier Ltd. All rights reserved.

1. Introduction

The clinical problem of congestive heart failure (CHF) is increasing in developed countries confronted with an aging society [1,2]. The morbidity of CHF increases with aging, as does mortality. Interestingly, approximately half of older patients with CHF show normal LV systolic but abnormal LV diastolic function. Recent studies have revealed that the prognosis of CHF associated with LV diastolic dysfunction is similar to that associated with LV systolic dysfunction [3]. However, therapeutic strategies aimed at improving LV diastolic dysfunction have not been established. In mammalian hearts, aging is associated with impaired cardiac relaxation [4–6]. Senescent cardiomyocytes are characterized by prolonged relaxation, diminished contraction velocity, a decrease in β -adrenergic response, and

increased myocardial stiffness. This impairment in diastolic function contributes, in part, to the increased incidence of CHF in the elderly [2].

Caloric restriction (CR) is the established intervention for which anti-aging effects have been proven scientifically [7,8]. CR can retard cellular senescence and attenuate the physiological decline in organ function. Hearts become more susceptible to various stresses with aging [5,6,9]. We have demonstrated that short-term (4 weeks) and prolonged (6 months) CR confers cardioprotection in aged and middle-aged rats, respectively [9,10]. These results indicate that CR retards cardiac senescence from the aspect of myocardial ischemic tolerance.

In addition, recent clinical studies have demonstrated that CR, when accompanied by significant body weight loss, has cardiac-specific effects that ameliorate LV diastolic function in healthy subjects [11,12], as well as in patients with type 2 diabetes mellitus (T2DM) [13]. Thus, clinical application of CR and the development of CR mimetics that can replicate the effects of CR have considerable potential as novel therapeutic approaches for the treatment of

* Corresponding author. Division of Geriatric Medicine, Department of Internal Medicine, Keio University School of Medicine, 35 Shinanomachi, Shinjuku-ku, Tokyo, Japan 160-8582. Tel.: +81 3 3353 1211x62915; fax: +81 3 5269 2468.

E-mail address: shimmura@sc.itc.keio.ac.jp (K. Shinmura).

patients with diastolic dysfunction. However, the exact mechanism(s) by which CR improves cardiac diastolic dysfunction remains unknown. Furthermore, how long-term CR modulates cardiac senescence has not been fully evaluated.

Therefore, the aim of the present study was to investigate the impact of long-term CR, which started at the age of 8-month-old and continued till the age of 30-month-old, on cardiac senescence, in particular the effects of CR on cardiac diastolic dysfunction associated with aging. Our results strongly suggest that long-term CR improves diastolic function in the senescent myocardium by ameliorating the age-associated deterioration in myocyte relaxation. Furthermore, our results indicate that attenuation of the decrease in sarcoplasmic reticulum calcium ATPase (SERCA) 2 with aging and enhanced autophagic flux are associated with functional improvements in the aged heart.

2. Materials and methods

All procedures in the present study conformed to the principles outlined in the *Guide for the Care and Use of Laboratory Animals* published by the US National Institutes of Health (NIH Publication No. 85-23, revised 1996) and were approved by the Institutional Animal Care and Use Committee of Keio University School of Medicine.

2.1. CR protocols

Seven-month-old male Fischer344 rats were obtained from Charles-River Japan. Rats were housed in individual cages according to institutional protocols at Keio University Experimental Animal Centre and fed ad libitum for 2 weeks with a modified semipurified diet A (Oriental Yeast Co.) (Supplemental Table 1). The average caloric intake was calculated from daily food intake over this 2-week period. After weaning, rats at the age of 8-month-old were randomly divided into two groups: AL rats ($n = 24$) continued to be fed ad libitum with control diet A, whereas CR rats ($n = 20$) were fed first with 90% of the average caloric intake during the 2-week run-in period (10% restriction), followed by 60% of the average caloric intake (40% energy reduction) till the age of 30-month-old using modified semipurified diets B and C. Modified semipurified diets B and C comprised the same calorie per weight, but were enriched in vitamins and minerals by 11% and 67%, respectively, compared with diet A (Supplemental Table 1). We reduced the daily calorie intake by decreasing food weight to 90% and 60% in the modified semipurified diets B and C, respectively. Three-month-old rats were used as the young controls (YC).

2.2. Echocardiography

At the age of 29-month-old, rats were anesthetized with 1.5% isoflurane inhalation and were anchored to a positionable platform in the supine position. Short axis echocardiography and Doppler echocardiographic measurements from the apical 4-chamber view were performed using the Vevo2100 echocardiography (VisualSonics). To obtain tissue Doppler imaging (TDI), sample volume was placed at the septal side of the mitral annulus and early (E') and late (A') diastolic mitral annular velocities were measured.

2.3. Histological examination

Senescence-associated β -galactosidase and lipofuscin were assessed in fresh frozen tissue sections. Briefly, cryostat sections were fixed in 3% formaldehyde and washed in phosphate-buffered saline (PBS) at room temperature. Slides were immersed in freshly prepared β -galactosidase staining solution [1 mg/mL X-gal in dimethylformamide, 40 mM citric acid, sodium phosphate (pH 6.0), 5 mM potassium ferrocyanide, 5 mM potassium ferricyanide, 150 mM

NaCl, and 2 mM $MgCl_2$] and incubated at 37 °C overnight. Stained slides were washed with PBS and counterstained with nuclear fast red. Other frozen tissue sections were fixed with 3% formaldehyde and viewed immediately by fluorescence microscopy with a 590 nm filter to assess autofluorescence of the myocardium [14]. Apoptotic cardiomyocytes were assessed using the ApopTag In Situ Apoptosis Detection Kit (Serologicals). Tissue sections were also stained with 4',6-diamidino-2-phenylindole (DAPI) to visualize nuclei. Percentage of TUNEL-positive myocytes was calculated by counting 10,000 nuclei in each group. Part of the heart was fixed overnight in 10% formalin at 4 °C, dehydrated with 70% ethanol, mounted in paraffin, and sectioned (5 μ m). Sections were stained with Hematoxylin and Eosin, Masson's trichrome, and Picosirius red (for fibrosis). The proportion of the fibrotic area was determined in slides stained with Picosirius red using a BIOREVO fluorescence microscope (BZ-9000, Keyence).

2.4. Lipofuscin assay

Heart tissue was ground in liquid nitrogen and homogenized in chloroform-methanol (1:20, w:v). After centrifugation, the chloroform-rich layer was mixed with the methanol. The fluorescence in this fraction was measured at an excitation wavelength of 350 nm and emission wavelength of 485 nm using a spectrofluorimeter [15]. Fluorescence intensity at 485 nm was expressed as units/100 mg tissue.

2.5. Isolation of cardiomyocytes

Ventricular cardiomyocytes were isolated from AL and CR rats as described previously [16] ($n = 6$, each). Briefly, hearts were mounted on a Langendorff apparatus and perfused with Tyrode solution containing 0.1 mM Ca^{2+} . Type II collagenase (Worthington) was then added to the perfusate. After 30 min, the hearts were taken down, ventricles minced, and myocytes dissociated by trituration. Subsequently, myocytes were filtered, centrifuged, and resuspended in MEM containing 1 mM Ca^{2+} . Myocytes were used within 6 h of isolation.

2.6. Measurement of $[Ca^{2+}]_i$

Myocytes were loaded at 22 °C with Fluo-4 AM (10 μ M; Molecular Probes) for 30 min, washed out, and then allowed to sit for a further 30 min to allow for intracellular deesterification. The cell fluorescence measurement was performed at room temperature using a Zeiss LSM-510 confocal microscope (5-Live mode). Laser excitation (488 nm) and emission (543 nm) were used for detecting Fluo-4 fluorescent signal [17]. Myocytes were incubated with 1.0 mM Ca^{2+} Tyrode solution and stimulated via platinum electrodes connected to a stimulator at a frequency of 1 Hz. Contraction amplitude and rates of contraction and relaxation were recorded online with a video edge-detection system and data acquisition software as described previously [17]. SR Ca^{2+} content was evaluated after rapid application of caffeine (10 mM) [18] and expressed as relative value of baseline F/F_0 .

2.7. SERCA activity

SERCA activity was assayed based on a pyruvate/NADH coupled reaction as described previously [19]. Oxidation of NADH was assessed at 37 °C in the membranous fractions from heart homogenate according to the difference between the total absorbance and basal absorbance at a wavelength of 340 nm. SERCA activity was expressed as nmol ATP/mg protein/min.

2.8. Western blotting

Total protein was extracted from frozen hearts. Equal amounts of total proteins (20–40 µg) were subjected to SDS-PAGE [9,10]. The primary antibodies used in the present study were anti-SERCA2, anti-phospholamban (PLB) (Affinity BioReagents), anti-phosphorylated PLB (Ser¹⁶) (ThermoScientific), anti-Na⁺-Ca²⁺ exchanger (NCX) 1 (Abcam), anti-troponin I, anti-phosphorylated troponin I (Ser^{23/24}), anti-Bcl-1, anti-mammalian target of rapamycin (mTOR), anti-phosphorylated mTOR (Ser²⁴⁴⁸), anti-p70 S6 kinase (S6K), anti-phosphorylated S6K (Thr³⁸⁹) (Cell Signaling Technology), anti-p16^{INK4a} (Santa Cruz Biotechnology), anti-light chain (LC) 3 (Medical & Biological Laboratories), and anti-glyceraldehydes 3-phosphate dehydrogenase (GAPDH) (Chemicon International). To assess protein carbonyls, protein extracts were reacted with 2,4-dinitrophenylhydrazine (DNPH) using the Oxyblot kit (Millipore) with a modification as described previously [20].

2.9. Chloroquine treatment

We evaluated the effect of chloroquine, a lysosomal protease inhibitor, on the expression of LC3-II using male 20-month-old rats fed with either AL or CR for 12 months. Alzet osmotic pump was implanted subcutaneously in the infrascapular region of either AL or CR rat. Chloroquine (10 mg/kg per day; Sigma) or saline vehicle was continuously administered for 4 weeks [14]. Three hearts from each group were used for Western immunoblotting.

2.10. Statistical analysis

Data are presented as the mean ± SEM. For intergroup comparisons, data were analyzed by one-way ANOVA, followed by Student's *t* tests for unpaired data with Bonferroni's correction. *P* < 0.05 was considered significant.

3. Results

3.1. Mortality

During the 22-month observation period, thirteen out of 24 rats in the AL group and 5 out of 20 rats in the CR group died. Thus, as expected, mortality was significantly less in the CR group than in the AL group (*P* < 0.05, Supplemental Fig. 1).

3.2. Echocardiographic findings

Aged hearts in the AL group exhibited an increase in LV mass and slightly reduced LV systolic parameters (Table 1). Although the E/A ratio was significantly higher in the AL group than that in the YC group, the deceleration time of the E wave and isovolumic relaxation time were longer in the AL group. In addition, TDI showed a remarkable decrease in peak E' velocity, a modest decrease in peak A' velocity, and a subsequent decrease in the E'/A' ratio in the AL group. These results indicate that LV diastolic function was severely impaired in aged hearts.

Echocardiographic parameters of LV systolic function were similar between AL and CR hearts (Table 1). CR attenuated the increase in LV mass with aging. As expected, long-term CR preserved LV diastolic function. The E/A ratio was similar between AL and CR hearts, but the deceleration time of the E wave and isovolumic relaxation time were significantly shorter in the CR group. TDI showed a higher E' velocity and a greater E'/A' ratio in the CR group.

3.3. Body weight and ventricular weight

Since rats were randomly divided into two groups, there was no difference in body weight (BW) at the age of 8-month-old between AL and CR [AL: 355 ± 5 (n = 16) vs. CR: 356 ± 8 (n = 14) g; n.s.]. BW at

Table 1
Echocardiographic parameters.

	YC	AL	CR
LV mass (mg)	587 ± 19 (n = 5)	691 ± 21 ⁺ (n = 8)	616 ± 12* (n = 10)
Ejection fraction (%)	76.8 ± 2.2 (n = 5)	71.4 ± 1.7* (n = 8)	69.8 ± 1.5* (n = 10)
% Fractional shortening	46.8 ± 1.7 (n = 5)	41.5 ± 1.8* (n = 8)	39.9 ± 1.4* (n = 10)
Peak E velocity (mm/s)	758 ± 24 (n = 5)	825 ± 35 (n = 6)	811 ± 22 (n = 8)
Deceleration time of the E wave (ms)	37.6 ± 1.3 (n = 5)	43.6 ± 1.5* (n = 6)	38.0 ± 1.3* (n = 8)
Peak A velocity (mm/s)	522 ± 21 (n = 5)	445 ± 34 (n = 6)	475 ± 23 (n = 8)
E/A ratio	1.46 ± 0.06 (n = 5)	1.88 ± 0.07* (n = 6)	1.73 ± 0.07* (n = 8)
Isovolumic relaxation time (ms)	22.8 ± 1.1 (n = 5)	33.3 ± 1.9* (n = 6)	27.5 ± 1.7** (n = 8)
Peak E' velocity (mm/s)	57.0 ± 1.9 (n = 5)	37.5 ± 2.1* (n = 6)	44.9 ± 2.7** (n = 8)
Peak A' velocity (mm/s)	55.7 ± 1.4 (n = 5)	46.7 ± 1.5* (n = 6)	47.6 ± 1.8* (n = 8)
E'/A' ratio	1.03 ± 0.04 (n = 5)	0.80 ± 0.04* (n = 6)	0.94 ± 0.02* (n = 8)
E/E' ratio	13.3 ± 0.3 (n = 5)	22.1 ± 0.4* (n = 6)	18.4 ± 0.4** (n = 8)

Data are the mean ± SEM. ⁺*P* < 0.05 vs. the YC group, **P* < 0.05 vs. the AL group. LV mass (uncorrected) (mg) = 1.053 × [(LVIDD + LVPWd + IVSd)³ - (LVIDD)³]. LV, left ventricular; LVIDD; LV internal diameter (diastole) (mm), LVPWd; LV posterior wall (diastole) (mm), IVSd; interventricular septum (diastole) (mm), YC, young controls; AL, rats fed the normal control diet ad libitum; CR, rats fed a caloric-restricted diet. Because of technical difficulty, Pulse-wave Doppler evaluation was achieved in 6 AL and 8 CR rats.

the age of 30-month-old was significantly heavier in the AL group than that in the CR group [AL: 348 ± 5 (n = 8) vs. CR: 290 ± 4 (n = 10) g; *P* < 0.05]. The ventricular weight was also heavier in the AL group [AL: 1.16 ± 0.02 (n = 8) vs. CR: 0.95 ± 0.02 (n = 10) g; *P* < 0.05], but the ratio of ventricular weight to BW was similar between AL and CR [AL: 0.326 ± 0.009 (n = 8) vs. CR: 0.329 ± 0.006 (n = 10) %; n.s.].

3.4. Histological examination and lipofuscin content

Histological analysis revealed that long-term CR significantly reduced cardiomyocyte size (Figs. 1(A and B)) and attenuated the accumulation of lipofuscin (Figs. 1(C and D)) and senescence-associated β-galactosidase (Fig. 1(E)). Aged AL rats showed an 8-fold increase in myocardial lipofuscin content, compared with young rats, and CR attenuated this increase by 40% (Fig. 1(D)). CR also reduced TUNEL-positive cells (Figs. 2(A and B)). However, the degree in cardiac fibrosis was similar between AL and CR (Figs. 2(C–E)).

3.5. Measurement of [Ca²⁺]_i

We isolated an average of 1 × 10⁷ ventricular myocytes, 80% of which are rod-shaped, from the young heart. In contrast, fewer isolated ventricular myocytes were obtained from aged rat heart. Of these, approximately one third were rod-shaped, indicating that aging attenuates the myocyte isolation yield. However, we did not find any difference in the myocyte isolation yield between the AL and CR aged hearts.

Fig. 3(A) shows the representative Fluo-4 line scan images, their corresponding [Ca²⁺]_i transients, and the traces of myocyte contractions in isolated myocytes obtained from AL and CR rats. There were no differences in peak amplitude of [Ca²⁺]_i transients, expressed as F/F₀ (Fig. 3(B)) between the two groups. In contrast, cardiomyocytes obtained from CR rats exhibited better Ca²⁺ uptake, as evidenced by a significantly decreased time to 50% relaxation (RT₅₀; Fig. 3(C)) and the tendency for a decrease of the τ of [Ca²⁺]_i decline in cardiomyocytes

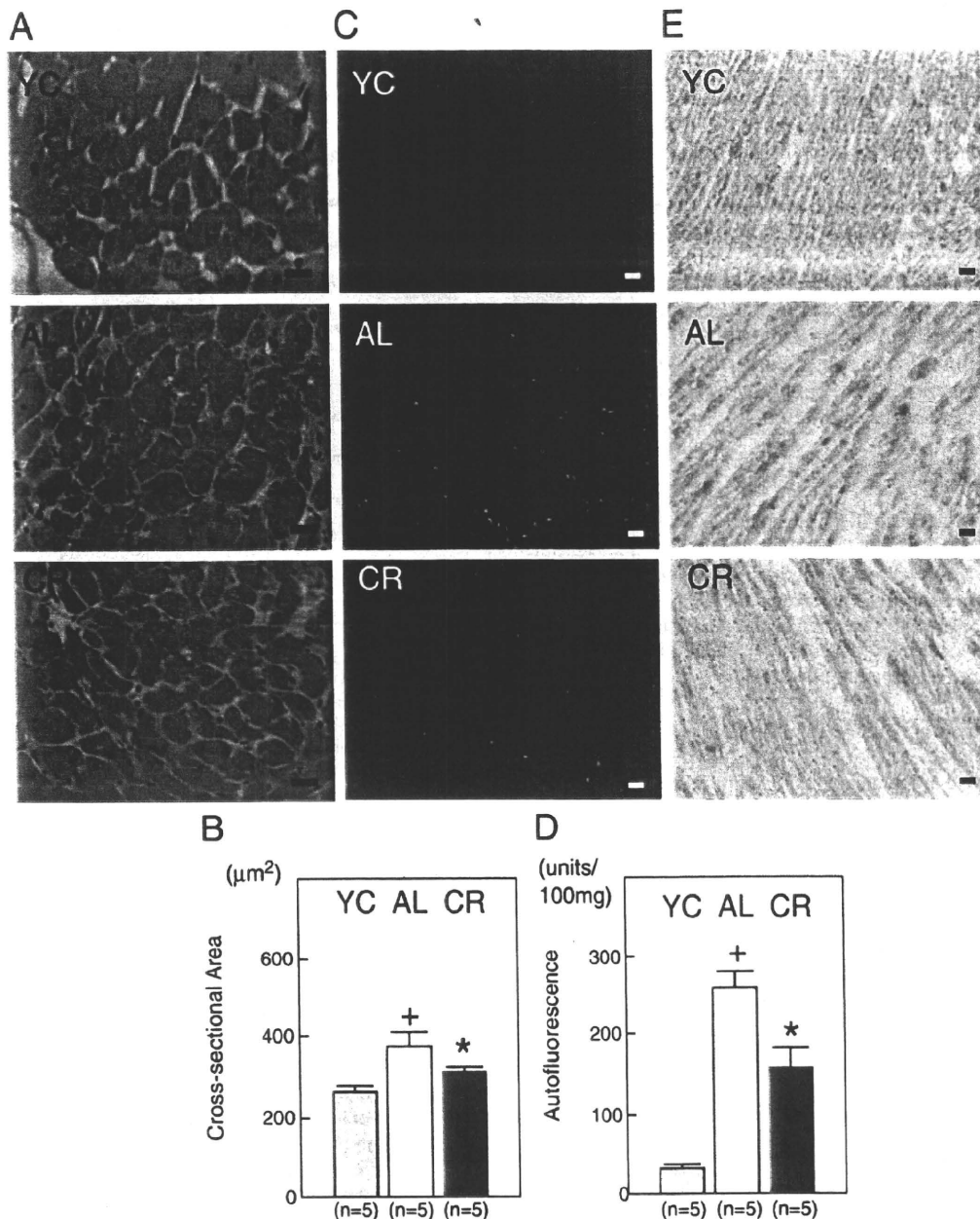


Fig. 1. Histological examination. (A) Hematoxylin and Eosin staining. (B) Cross-sectional view of cardiomyocytes in AL and CR rats. (C) Lipofuscin. (D) Myocardial lipofuscin content. (E) Senescence-associated β -galactosidase. Bar: 50 μ m. YC: young controls, AL: rats fed the normal control diet ad libitum, CR: rats fed a caloric-restricted diet. Data are the mean \pm SEM. Quantitative data are pooled data from 5 AL hearts and 5 CR hearts. $^+P < 0.05$ vs. the YC group. $^*P < 0.05$ vs. the AL group.

obtained from CR rats (Fig. 3(D)). Corresponding with these results, cardiomyocytes obtained from CR rats exhibited better relaxation, as evidenced by a decreased RT_{50} (Fig. 3(F)), although there was no difference in fractional shortening between the groups (Fig. 3(E)) These results suggested that better Ca^{2+} uptake results in better myocyte relaxation in hearts from CR rats. However, CR did not increase the SR Ca^{2+} content in the aged heart (Fig. 3(G)).

3.6. SERCA activity

SERCA activity significantly decreased with aging, but CR enhanced SERCA activity by 30% in the aged heart {YC: 205 ± 6 (n=5), AL: 88 ± 5 (n=3), CR: 114 ± 6 (n=5) nmol/mg protein/min; $P < 0.05$ YC vs. AL, $P < 0.05$ AL vs. CR}.

3.7. Western immunoblotting

The oxyblot analysis demonstrated that protein carbonyls increased with aging and CR attenuated this increase (Fig. 4(A)), suggesting that long-term CR reduces oxidative stress in the aged heart.

Expression of senescence markers was compared among three groups. The expression of p16^{INK4a} increased with aging in the AL group, and this increase was attenuated in the CR group (Figs. 4(B and C)). In contrast, CR failed to attenuate the decrease in phosphorylated troponin I at the Ser^{23/24} residue (P-troponin I) with aging (Figs. 4(B and D)). It is well known that the expression of SERCA2 protein decreases with aging and this phenomenon contributes, in part, to impaired cardiac diastolic dysfunction associated with aging [5,21]. In the present study, long-term CR significantly attenuated the decrease

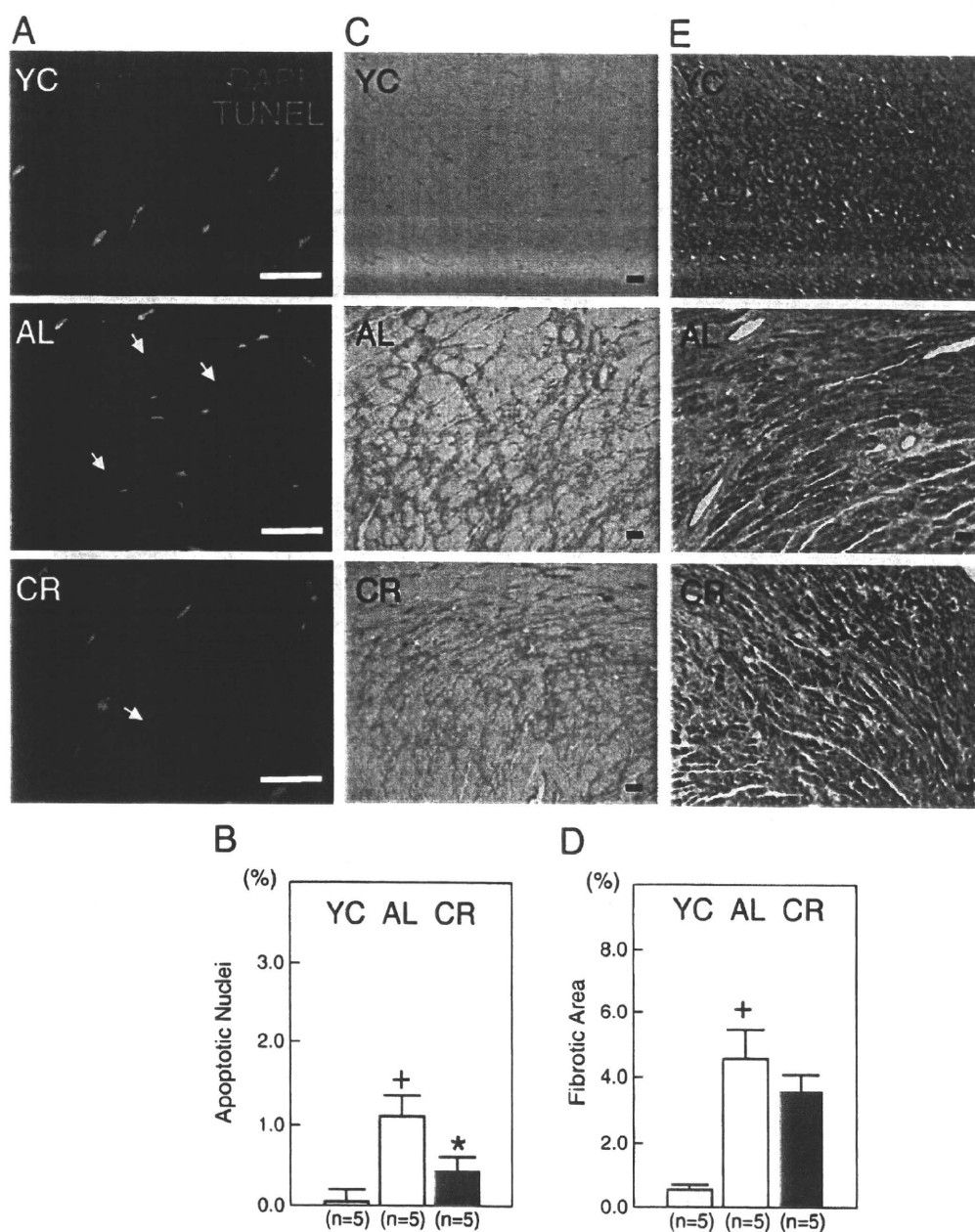


Fig. 2. Histological examination. (A) TUNEL staining. (B) Percentage of TUNEL-positive nuclei to total nuclei in AL and CR rats. (C) Picosirius red staining. (D) Percentage of fibrotic area to LV area in AL and CR rats calculated in Picosirius red staining. (E) Masson's trichrome staining. Bar: 50 μ m. Data are the mean \pm SEM. Quantitative data are pooled data from 5 AL hearts and 5 CR hearts. + $P < 0.05$ vs. the YC group. * $P < 0.05$ vs. the AL group.

in SERCA2 protein expression, but had no effect on the expression of NCX1 and phosphorylated and total PLB (Figs. 4(B and E)), both of which are involved in Ca^{2+} uptake during myocyte relaxation.

The amount of conjugated LC3 (LC3-II) correlates with the number of autophagosomes. More recently, it was reported that an increase in the ratio of LC3-II to the cytosolic form of LC3 (LC3-I) is a better biochemical marker by which to assess ongoing autophagy [22]. The expression levels of LC3-II and the LC3-II/LC3-I ratio decreased with aging (Figs. 5(A–C)). Although the expression levels of LC3-I were similar between AL and CR, the expression of LC3-II was significantly higher in hearts from CR rats, consequently increasing the ratio of LC3-II to LC3-I comparable with that in young hearts (Figs. 5(A–C)). In addition, the expression levels of beclin1 were higher in hearts from CR rats compared with that in hearts from AL rats (Figs. 5(A and D)).

To examine the possible involvement of the mTOR pathway as an upstream signaling of enhanced autophagy, the expression levels of phosphorylated and total mTOR and S6K were compared among three groups. There was no difference in the expression levels of phosphorylated and total mTOR and S6K between young and aged hearts (Fig. 6). However, long-term CR significantly attenuated phosphorylated forms of mTOR and S6K without affecting total protein levels (Fig. 6).

To clarify which mechanism is mainly responsible for the increase in LC3-II expression in the CR group, enhanced autophagic influx or lysosomal dysfunction, we evaluated the effects of chloroquine on the expression of LC3-II using male 20-month-old rats fed with either AL or CR for 12 months (Fig. 7). Because autophagic activity is represented by the flux in autophagosomes, this can be estimated by comparing LC3-II expression in the presence of the lysosomal protease inhibitor chloroquine [23]. Chloroquine treatment resulted

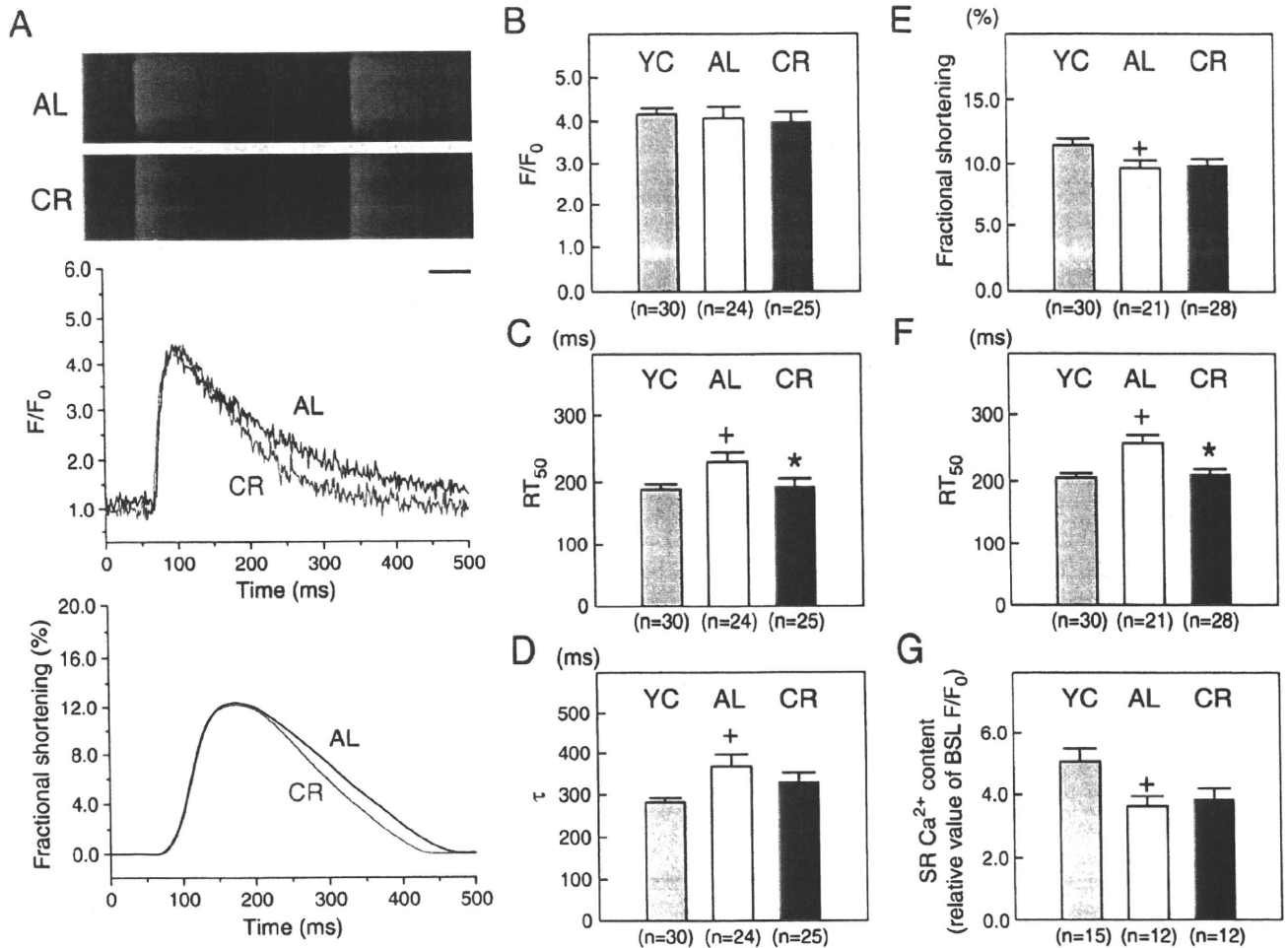


Fig. 3. Measurement of $[Ca^{2+}]_i$ and myocyte contractions in isolated myocytes. (A) Representative Fluoro-4 line scan images and traces of Ca^{2+} transients and myocyte contractions in isolated myocytes obtained from AL and CR rats. (B) Ratio of peak to basal $[Ca^{2+}]_i$ amplitude, expressed as F/F_0 . (C) Time to 50% relaxation in Ca^{2+} transient (RT_{50}). (D) τ of $[Ca^{2+}]_i$ decline. (E) Fractional shortening. (F) Time to 50% relaxation in myocyte contraction (RT_{50}). (G) SR Ca^{2+} content. Data are the mean \pm SEM. ⁺ $P < 0.05$ vs. the YC group. ^{*} $P < 0.05$ vs. the AL group.

in a significant increase in LC3-II expression in both the AL and CR groups. However, the LC3-II/LC3-I ratio remained higher in hearts from CR rats compared with AL rats, suggesting that autophagic flux is enhanced in hearts from CR rats.

4. Discussion

The major findings of the present study are: (1) long-term CR improves LV diastolic function without affecting LV systolic function; (2) long-term CR attenuates myocyte apoptosis and the cardiac expression of markers of senescence, such as β -galactosidase, lipofuscin, and p16^{INK4a}; (3) long-term CR fails to reduce cardiac fibrosis and to prevent decreases in p-troponin I and p-phospholamban; (4) long-term CR attenuates the decrease in SERCA2 protein and ameliorates age-associated deterioration of intracellular Ca^{2+} handling; (5) long-term CR suppresses the mTOR pathway; and (6) long-term CR enhances autophagic flux in the heart.

The impact of long-term CR on cardiovascular senescence has not been fully evaluated. Taffet et al. reported that long-term CR improved age-associated changes in late diastolic function in mice [24]. More recently, Barger et al. demonstrated that CR prevents the age-related increase in isovolumic relaxation time and the decrease in the myocardial performance index in mice [25]. In the present study, long-term CR improved LV diastolic function without affecting LV systolic function in senescent rats. Furthermore, our results suggest that long-term CR ameliorates the age-associated deterioration of

early diastolic function by maintaining the function of the sarcoplasmic reticulum (SR). Our findings differ from those of Taffet et al. [24] because those authors found no improvement in early diastolic cardiac function in mice. However, our results are consistent with those of Seymour et al. [26], who reported that CR improves cardiac remodeling and diastolic dysfunction in Dahl-SS rats.

The age-associated impairment in cardiac diastolic function is complicated. There is ample evidence from studies using senescent rats implicating slowed cardiac relaxation and altered Ca^{2+} handling in the impaired diastolic function [5,6,21]. In particular, impaired SERCA activity, which is mainly responsible for controlling $[Ca^{2+}]_i$ by taking up Ca^{2+} into the SR during relaxation, has been identified as contributing to the abnormalities in cardiac relaxation. The decrease in SR Ca^{2+} uptake during relaxation, which results in prolonged contraction, has been shown to be associated with decreased SERCA2 content and activity in experimental models of senescence [5,6,21]. More recently, SERCA2a protein levels have been reported to be significantly decreased in the senescent human myocardium [27]. Changes in active cardiac relaxation impact on early diastolic parameters, such as peak E velocity and E deceleration time, rather than on late diastolic parameters [28]. In the present study, attenuation of the decrease in SERCA2 protein and its activity in senescent CR hearts was associated with an improvement in RT_{50} and τ , indicators of a decline in $[Ca^{2+}]_i$. Schmidt et al. [21] demonstrated that overexpression of SERCA2a by gene transfer improved diastolic function in senescent rat hearts. Therefore, we speculate that long-

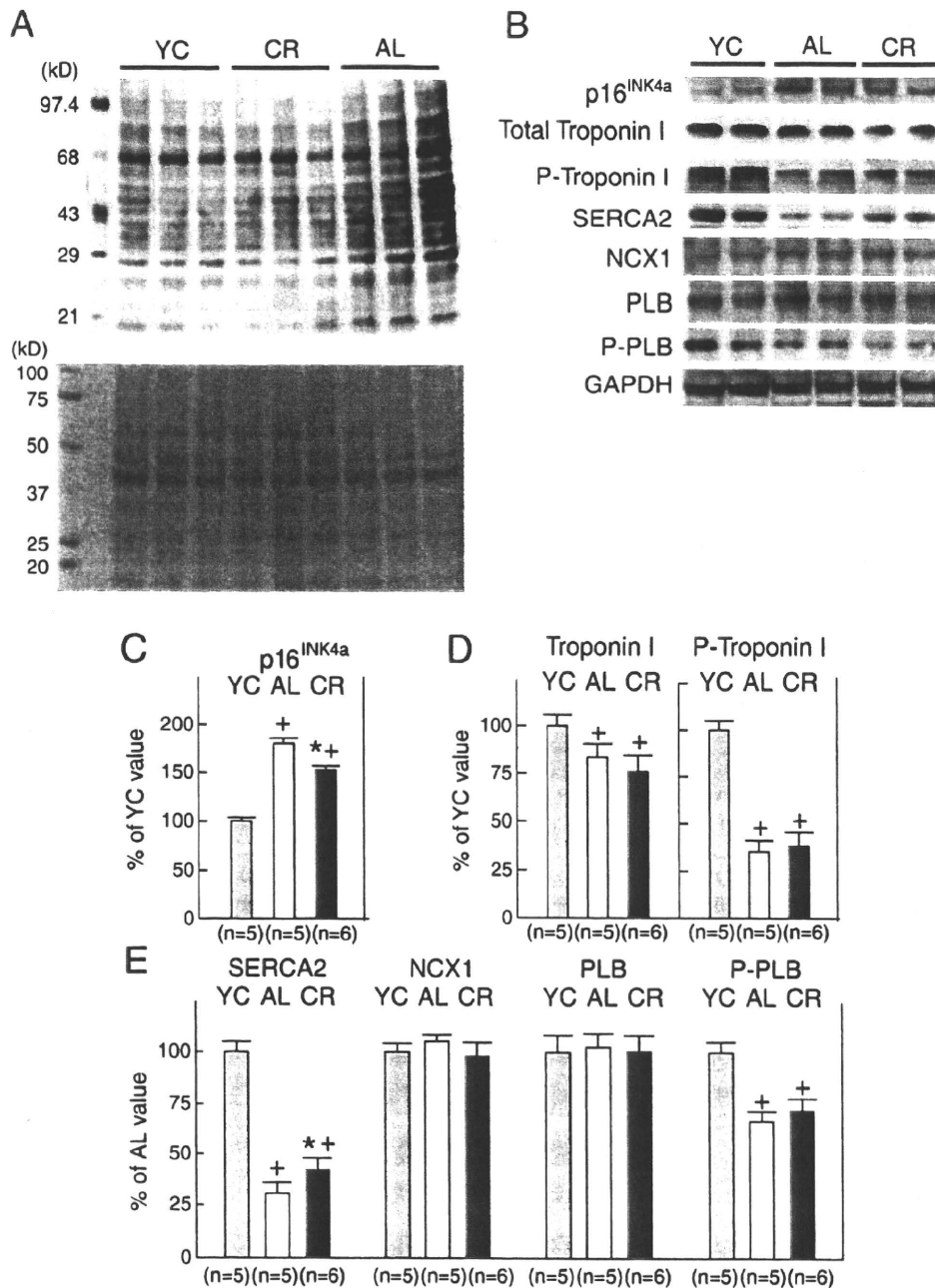


Fig. 4. Oxyblots and Western immunoblotting for senescence markers and proteins related to Ca^{2+} uptake during relaxation. (A) Representative oxyblots showing protein carbonyls (upper panel) and the corresponding Ponceau S staining (lower panel). (B) Representative Western immunoblots showing the expression of p16^{INK4a}, total troponin I, troponin I phosphorylated at the Ser^{23/24} residue (P-troponin I), sarcoplasmic reticulum calcium ATPase (SERCA) 2, Na^{+} - Ca^{2+} exchanger (NCX) 1, total phospholamban (PLB), phospholamban phosphorylated at the Ser¹⁶ residue (P-PLB), and glyceraldehydes 3-phosphate dehydrogenase (GAPDH). (C) Densitometric analysis of p16^{INK4a}. (D) Densitometric analysis of total troponin I and P-troponin I. (E) Densitometric analysis of SERCA2, NCX1, total PLB and P-PLB. Densitometric measurements of protein immunoreactivity are expressed as a percentage of the average value measured in YC rats. Data are the mean \pm SEM. ⁺ $P < 0.05$ vs. the YC group. ^{*} $P < 0.05$ vs. the AL group. YC: young controls.

term CR ameliorates the age-associated deterioration of myocyte relaxation by attenuating the decrease in SERCA2 protein with aging.

It was demonstrated recently that mice with cardiac-specific excision of the SERCA2 gene present only moderate contractile dysfunction because of an SR-independent compensatory mechanism [18]. These results might argue against a major role of SERCA2 for diastolic dysfunction. Similarly, enhanced SERCA2 activity is usually associated with enhanced Ca^{2+} transient and contractility [29]. However, these findings were not consistent with our results. In contrast to cardiac-specific SERCA2-deficient mice, the decrease in SERCA2 proteins might develop very slowly in aged rats. The

induction of cardiomyocyte-specific *Serca2* gene excision resulted in less than 5% SERCA2 protein expression [18], although the expression levels of SERCA2 protein in the AL aged heart remained at 30% of levels in the young heart (Fig. 4(E)). Thus, based on the results of Anderson et al. [18], we propose that the change in SERCA2 expression impacted markedly on myocyte Ca^{2+} homeostasis so the compensatory mechanism was strongly invoked in cardiomyocyte-specific *Serca2*-deficient mice. As shown in Figs. 3 and 4, there was no difference in peak Ca^{2+} transient or in expression levels of Na^{+} - Ca^{2+} exchanger between the AL and CR hearts, suggesting that the compensatory mechanism regarding SR Ca^{2+} handling was not sufficiently evoked in

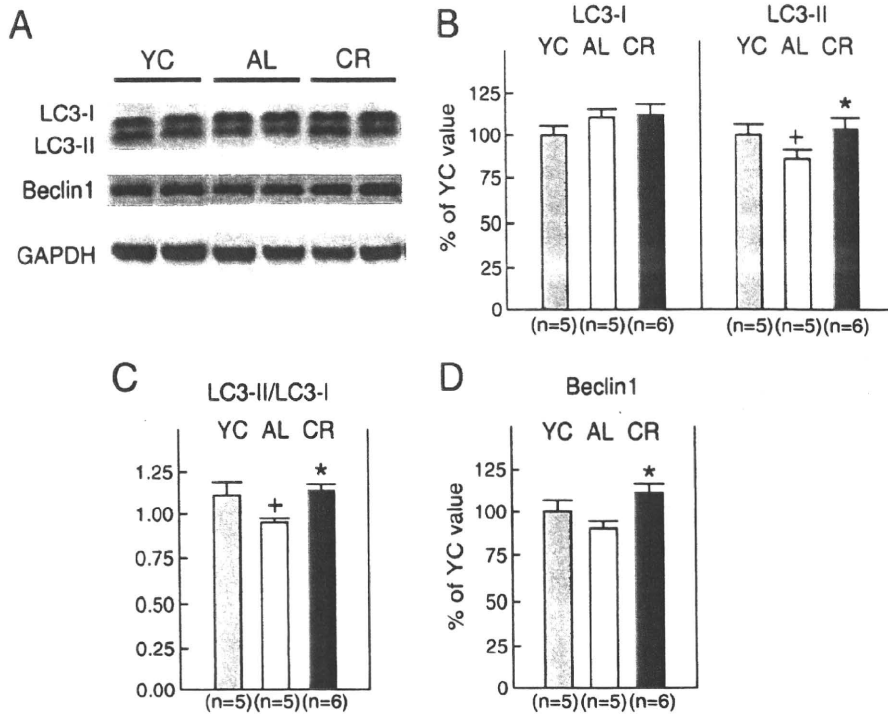


Fig. 5. Western immunoblotting for light chain 3 (LC3) and beclin1. (A) Representative Western immunoblots showing the expression of conjugated (LC3-II), cytosolic (LC3-I) LC3, beclin1 and GAPDH. (B) Densitometric analysis of LC3-I and LC3-II. (C) The LC3-II/LC3-I ratio. (D) Densitometric analysis of beclin1. Densitometric measurements of protein immunoreactivity are expressed as a percentage of the average value measured in YC rats. Data are the mean \pm SEM. ⁺P<0.05 vs. the YC group. ^{*}P<0.05 vs. the AL group. YC: young controls.

the aged heart. Although CR enhanced SERCA2 protein expression and activity in the aged heart, there was no difference in the SR Ca²⁺ content between myocytes obtained from the AL and CR hearts.

Overall, we speculate that CR could improve SR Ca²⁺ uptake rate during myocyte relaxation, but would not impact sufficiently to increase total SR Ca²⁺ content because the magnitude of the increase

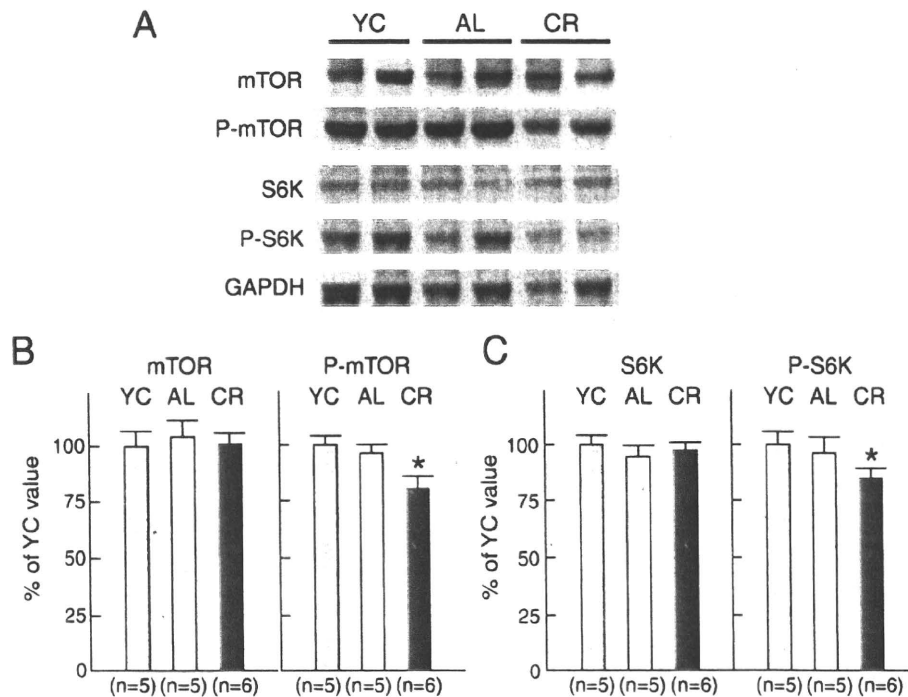


Fig. 6. Western immunoblotting for mammalian target of rapamycin (mTOR) signalings. (A) Representative Western immunoblots showing the expression of total mTOR, mTOR phosphorylated at the Ser²⁴⁴ residue (P-mTOR), total p70 S6 kinase (S6K), S6K phosphorylated at the Thr³⁸⁹ residue (P-S6K) and GAPDH. (B) Densitometric analysis of total mTOR and P-mTOR. (C) Densitometric analysis of total S6K and P-S6K. Densitometric measurements of protein immunoreactivity are expressed as a percentage of the average value measured in YC rats. Data are the mean \pm SEM. ^{*}P<0.05 vs. the AL group. YC: young controls.

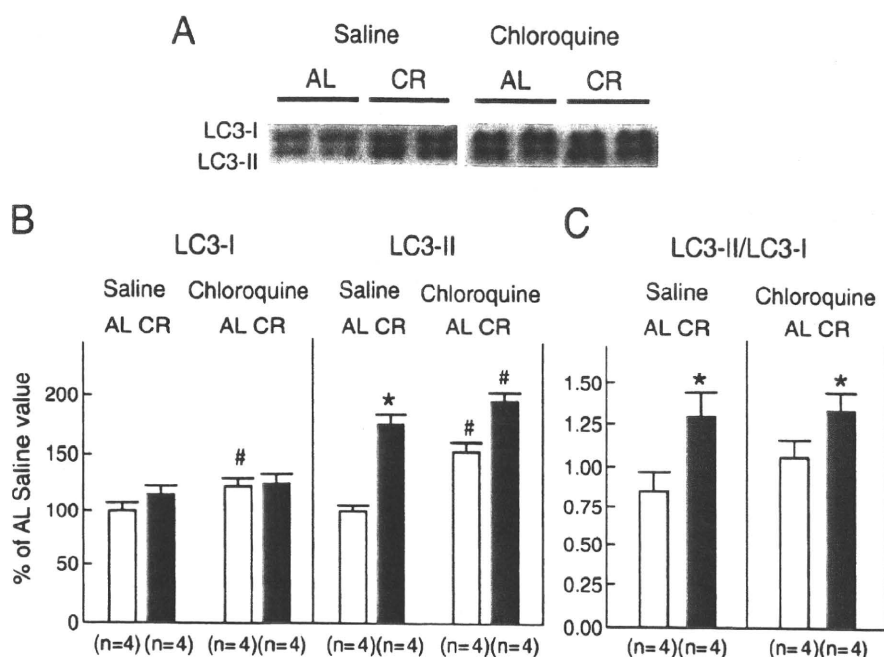


Fig. 7. Western immunoblotting for LC3 in 20-month-old AL and CR rats treated with either saline or chloroquine. (A) Representative Western immunoblots showing the expression of LC3-I and LC3-II. (B) Densitometric analysis of LC3-I and LC3-II. (C) The LC3-II/LC3-I ratio. Densitometric measurements of protein immunoreactivity are expressed as a percentage of the average value in AL rats treated with saline. Data are the mean \pm SEM. * $P < 0.05$ vs. the AL group; # $P < 0.05$ vs. the corresponding saline-treated group.

in SERCA2 protein by CR was only slight compared with previous reports in which SERCA2 was overexpressed in the failing human heart [29] and the senescent rat heart [21]. Therefore, enhanced SERCA2 protein expression by CR was not associated with enhanced Ca^{2+} transient and contractility in the present study.

In addition, decreased size of cardiomyocytes might contribute to the amelioration of LV diastolic dysfunction in CR rats. Myocyte hypertrophy is associated with changes in the cytoskeletal proteins that could alter the microtubule architecture and heighten organization of sarcomeres within individual myocytes. An increased collagen volume fraction, larger cardiomyocyte diameter, and higher resting cardiomyocyte tension have been correlated with LV diastolic stiffness [30]. With aging, the myosin heavy chain isoform shifts from α to β in the rodent heart [5]. Lieber et al. [31] demonstrated that α - and β -tubulin were significantly increased and desmin was decreased in aged rats, and this finding might explain the observed cardiac dysfunction with aging. Posttranslational modification of myofilament proteins including titin might play an important role in diastolic heart failure associated with aging [32]. Our results indicated that cardiomyocyte responsiveness to Ca^{2+} estimated from the relationship between Ca^{2+} transient and myocyte shortening is similar between isolated myocytes obtained from AL and CR rat hearts (Fig. 3). This finding supports our hypothesis that inhibiting the SERCA2 expression decline is a major factor in preserving LV diastolic function by CR. However, it is also possible that CR affects these age-associated alterations in cytoskeletal proteins. Thus, we would evaluate the changes in myofilament proteins in aged rats treated with long-term CR in future studies.

The accumulation of myocardial collagen and extracellular matrix increases with aging, contributing to increased cardiac fibrosis, myocardial stiffness, and cardiac diastolic dysfunction [5,6]. Dhahbi et al. demonstrated that long-term CR reduced myocardial collagen and extracellular matrix content and attenuated cardiac fibrosis associated with aging [33]. Thus, CR-induced changes in cardiac connective tissue may contribute, in part, to the amelioration of diastolic function, especially late diastolic function, as observed by Taffet et al. [24]. However, we could not find a

significant decrease in cardiac fibrosis in CR rat hearts (Figs. 2(C–E)). We speculate that the discrepancy between the study of Taffet et al. [24] and the present study could be due, at least in part, to species differences and large individual variations with physiological aging. In addition, this discrepancy could be related to species functional differences including the metabolic rate and heart rate. These differences must be considered with regard to fibrosis, extracellular matrix composition, and fibrosis–renin–angiotensin–aldosterone system (RAS) interactions. Recent investigations revealed an essential role of RAS on the development of cardiac fibrosis with aging. Both pharmacological inhibition of RAS and targeted disruption of the angiotensin type 1 receptor prolonged lifespan and significantly attenuated cardiac fibrosis associated with aging [34,35]. Thus, our results may suggest that CR is not sufficient to suppress the activation of RAS with aging. Further investigations are necessary to clarify this issue.

The mechanisms by which long-term CR retards cellular senescence and attenuates the physiological decline of organ function have not been fully elucidated. Aging occurs, in part, as a result of the accumulation of oxidative damage caused by oxidative free radicals that are generated continuously during the course of metabolic processes [5,6,8]. In contrast, CR decreases the age-associated accumulation of oxidative damage to lipids, proteins, and DNA [7,8,26]. In the present study, the expression of protein carbonyls was less in CR hearts compared with AL hearts (Fig. 4A). Thus, it is possible that long-term CR retards cellular senescence and ameliorates age-related functional decline by attenuating oxidative damage in the aged heart. However, there is still no direct evidence that attenuation of oxidative damage is the primary means by which CR prevents cardiac senescence.

Another possible mechanism by which long-term CR retards cardiac senescence is enhancement of autophagy. Although the role of autophagy under stressed conditions is yet to be elucidated, autophagy under basal conditions plays a housekeeping role in the turnover of cytoplasmic constituents [22,23]. Thus, enhanced autophagy during CR is considered to be protective by degrading and removing damaged organelles and accumulated protein

aggregates. Our results indicate that autophagic flux is enhanced in CR hearts and this finding is consistent with previous studies [36]. Inuzuka et al. demonstrated that suppression of phosphoinositide 3-kinase preserved cardiac function and attenuated the expression of senescence makers associated with enhanced autophagy [14]. Temporal inhibition of autophagy in tamoxifen-treated *Atg5^{lox/lox}; MerCreMer⁺* mice leads to LV hypertrophy, LV dilatation, and contractile dysfunction [37]. Because autophagy is not inhibited but is only somewhat imperfect in the aged heart [38], the accumulation of impaired SR and mitochondria is sublethal and may result in diastolic dysfunction only. Impaired autophagy in the aged heart may contribute, in part, to the accumulation of lipofuscin, further inhibiting autophagy [38]. In the present study, long-term CR attenuated the accumulation of lipofuscin, suggesting that long-term CR disrupts this cycle in the aged heart. In addition, we demonstrated that enhanced autophagy was associated with suppressed the mTOR pathway in the hearts. Activation of mTOR exerts a negative regulatory effect on the induction of autophagy [39]. Rapamycin, an inhibitor of mTOR, has been shown to regress existing cardiac hypertrophy induced by pressure overload [40] and, more recently, has been reported to prolong lifespan in mice if it was started after middle age [41]. However, the exact mechanism by which enhanced autophagy preserves LV diastolic function remains to be resolved in the future. Further studies are also necessary to determine the upstream pathways of mTOR such as AMP-activated protein kinase and phosphoinositide 3-kinase/Akt in CR hearts.

Meyer et al. demonstrated that CR was beneficial for LV diastolic function in humans, because the E/A ratio was greater in their CR group than in the group fed a Western diet, with no significant differences in LV systolic function between them [11]. Meyer et al. speculated that CR has a beneficial effect on LV diastolic function by lowering systolic blood pressure and decreasing systemic inflammation and probably myocardial fibrosis. Although it is difficult to compare the data from human studies with those obtained in experimental animal models, it seems reasonable to assume that a common mechanism is involved in CR-induced improvements in LV diastolic function. Recent investigations suggest that myocardial triglyceride content is an independent predictor of diastolic function in the elderly [42] and patients with T2DM [43]. The decrease in myocardial triglyceride content produced by CR was associated with an improvement in LV diastolic function [13]. It is plausible that enhanced autophagy contributes to the degradation of potentially toxic fatty acid intermediates.

In conclusion, the present study has demonstrated that long-term CR partially retards cardiac senescence and attenuates the functional decline of the aged heart. Because the increased incidence of CHF in the elderly is becoming an urgent health problem in developed countries [2], CR and CR mimetics may provide a novel therapeutic strategy for reducing patients with LV diastolic dysfunction. Although we cannot yet conclude that there is a common mechanism underlying the effects of CR in humans and animal experimental models, the results of the present study do suggest the usefulness of enhanced autophagy as a novel therapeutic strategy to maintain cardiac diastolic function.

Supplementary materials related to this article can be found online at doi:10.1016/j.jmcc.2010.10.018.

Acknowledgments

The authors thank Drs. Roberto Bolli and Shin-ichiro Imai for critical discussions and Mr. Yoshiharu Tsuru, Ms. Yoshiko Miyake, and Ms. Naoko Higashijima for their technical assistance.

This study was supported in part by the Vehicle Racing Commemorative Foundation (2007–2009) (to Dr. Shinmura and Dr. Sano), by the Nateglinide Memorial Toyoshima Research and Education Fund (2007), and by the Novartis Foundation for Gerontological Research (2008) (to Dr. Shinmura). There is no relationship with industry.

References

- [1] Haan MN, Selby JV, Quesenberry Jr CP, Schmittiel JA, Fireman BH, Rice DP. The impact of aging and chronic disease on use of hospital and outpatient services in a large HMO: 1971–1991. *J Am Geriatr Soc* 1997;45:667–74.
- [2] Lakatta EG, Levy D. Arterial and cardiac aging: major shareholders in cardiovascular disease enterprises: part II: the aging heart in health: links to heart disease. *Circulation* 2003;107:346–54.
- [3] Chatterjee K, Massie B. Systolic and diastolic heart failure: differences and similarities. *J Card Fail* 2007;13:569–76.
- [4] Boluyt MO, Converso K, Hwang HS, Mikkor A, Russell MW. Echocardiographic assessment of age-associated changes in systolic and diastolic function of the female F344 rat heart. *J Appl Physiol* 2004;96:822–8.
- [5] Lakatta EG. Arterial and cardiac aging: major shareholders in cardiovascular disease enterprises: part III: cellular and molecular clues to heart and arterial aging. *Circulation* 2003;107:490–7.
- [6] Weisfeldt M. Aging, changes in the cardiovascular system, and responses to stress. *Am J Hypertens* 1998;11:415–55.
- [7] Heilbronn LK, Ravussin E. Calorie restriction and aging: review of the literature and implications for studies in humans. *Am J Clin Nutr* 2003;78:361–9.
- [8] Masoro EJ. Overview of caloric restriction and ageing. *Mech Ageing Dev* 2005;126:913–22.
- [9] Shinmura K, Tamaki K, Bolli R. Short-term caloric restriction improves ischemic tolerance independent of opening of ATP-sensitive K⁺ channels in both young and aged hearts. *J Mol Cell Cardiol* 2005;39:285–96.
- [10] Shinmura K, Tamaki K, Bolli R. Impact of 6-mo caloric restriction on myocardial ischemic tolerance: possible involvement of nitric oxide-dependent increase in nuclear Sirt1. *Am J Physiol Heart Circ Physiol* 2008;295:H2348–55.
- [11] Meyer TE, Kovacs SJ, Ehsani AA, Klein S, Holloszy JO, Fontana L. Long-term caloric restriction ameliorates the decline in diastolic function in humans. *J Am Coll Cardiol* 2006;47:398–402.
- [12] Riordan MM, Weiss EP, Meyer TE, Ehsani AA, Racette SB, Villareal DT, et al. The effects of caloric restriction- and exercise-induced weight loss on left ventricular diastolic function. *Am J Physiol Heart Circ Physiol* 2008;294:H1174–82.
- [13] Hammer S, Snel M, Lamb HJ, Jazet IM, van der Meer RW, Pijl H, et al. Prolonged caloric restriction in obese patients with type 2 diabetes mellitus decreases myocardial triglyceride content and improves myocardial function. *J Am Coll Cardiol* 2008;52:1006–12.
- [14] Inuzuka Y, Okuda J, Kawashima T, Kato T, Niizuma S, Tamaki Y, et al. Suppression of phosphoinositide 3-kinase prevents cardiac aging in mice. *Circulation* 2009;120:1695–703.
- [15] Savitha S, Naveen B, Panneerselvam C. Carnitine and lipoate ameliorates lipofuscin accumulation and monoamine oxidase activity in aged rat heart. *Eur J Pharmacol* 2007;574:61–5.
- [16] Ishida H, Genka C, Hirota Y, Nakazawa H, Barry WH. Formation of planar and spiral Ca²⁺ waves in isolated cardiac myocytes. *Biophys J* 1999;77:2114–22.
- [17] Picht E, DeSantiago J, Huke S, Kaetzel MA, Dedman JR, Bers DM. CaMKII inhibition targeted to the sarcoplasmic reticulum inhibits frequency-dependent acceleration of relaxation and Ca²⁺ current facilitation. *J Mol Cell Cardiol* 2007;42:196–205.
- [18] Andersson KB, Birkeland JA, Finsen AV, Louch WE, Sjaastad I, Wang Y, et al. Moderate heart dysfunction in mice with inducible cardiomyocyte-specific excision of the *Serca2* gene. *J Mol Cell Cardiol* 2009;47:180–7.
- [19] Hajjar RJ, Kang JX, Gwathmey JK, Rosenzweig A. Physiological effects of adenoviral gene transfer of sarcoplasmic reticulum calcium ATPase in isolated rat myocytes. *Circulation* 1997;95:423–9.
- [20] Divald A, Kivity S, Wang P, Hochhauser E, Roberts B, Teichberg S, Gomes AV, Powell SR. Myocardial ischemic preconditioning preserves postsischemic function of the 26S proteasome through diminished oxidative damage to 19S regulatory particle subunits. *Circ Res* 2010;106:1829–38.
- [21] Schmidt U, del Monte F, Miyamoto MI, Matsui T, Gwathmey JK, Rosenzweig A, et al. Restoration of diastolic function in senescent rat hearts through adenoviral gene transfer of sarcoplasmic reticulum Ca(2+)-ATPase. *Circulation* 2000;101:790–6.
- [22] Mizushima N, Yoshimori T. How to interpret LC3 immunoblotting. *Autophagy* 2007;3:542–5.
- [23] Iwai-Kanai E, Yuan H, Huang C, Sayen MR, Perry-Garza CN, Kim L, et al. A method to measure cardiac autophagic flux in vivo. *Autophagy* 2008;4:322–9.
- [24] Taffet GE, Pham TT, Hartley CJ. The age-associated alterations in late diastolic function in mice are improved by caloric restriction. *J Gerontol A Biol Sci Med Sci* 1997;52:B285–90.
- [25] Barger JL, Kayo T, Vann JM, Arias EB, Wang J, Hacker TA, et al. A low dose of dietary resveratrol partially mimics caloric restriction and retards aging parameters in mice. *PLoS ONE* 2008;3:e2264.
- [26] Seymour EM, Parikh RV, Singer AA, Bolling SF. Moderate calorie restriction improves cardiac remodeling and diastolic dysfunction in the Dahl-S5 rat. *J Mol Cell Cardiol* 2006;41:661–8.
- [27] Cain BS, Meldrum DR, Joo KS, Wang JF, Meng X, Cleveland Jr JC, et al. Human SERCA2a levels correlate inversely with age in senescent human myocardium. *J Am Coll Cardiol* 1998;32:458–67.
- [28] Nishimura RA, Abel MD, Hatle LK, Holmes Jr DR, Housmans PR, Ritman EL, et al. Significance of Doppler indices of diastolic filling of the left ventricle: comparison with invasive hemodynamics in a canine model. *Am Heart J* 1989;118:1248–58.
- [29] del Monte F, Harding SE, Schmidt U, Matsui T, Kang ZB, Dec GW, et al. Restoration of contractile function in isolated cardiomyocytes from failing human hearts by gene transfer of SERCA2a. *Circulation* 1999;100:2308–11.

- [30] Borbely A, van der Velden J, Papp Z, Bronzwaer JG, Edes I, Stienen GJ, et al. Cardiomyocyte stiffness in diastolic heart failure. *Circulation* 2005;111:774–81.
- [31] Lieber SC, Qiu H, Chen L, Shen YT, Hong C, Hunter WC, et al. Cardiac dysfunction in aging conscious rats: altered cardiac cytoskeletal proteins as a potential mechanism. *Am J Physiol Heart Circ Physiol* 2008;295:H860–6.
- [32] Granzier H, Wu Y, Siegfried L, LeWinter M. Titin: physiological function and role in cardiomyopathy and failure. *Heart Fail Rev* 2005;10:211–23.
- [33] Dhahbi JM, Tsuchiya T, Kim HJ, Mote PL, Spindler SR. Gene expression and physiologic responses of the heart to the initiation and withdrawal of caloric restriction. *J Gerontol A Biol Sci Med Sci* 2006;61:218–31.
- [34] Basso N, Cini R, Pietrelli A, Ferder L, Terragno NA, Inserra F. Protective effect of long-term angiotensin II inhibition. *Am J Physiol Heart Circ Physiol* 2007;293:H1351–8.
- [35] Benigni A, Corna D, Zoja C, Sonzogni A, Latini R, Salio M, et al. Disruption of the Ang II type 1 receptor promotes longevity in mice. *J Clin Invest* 2009;119:524–30.
- [36] Wohlgemuth SE, Julian D, Akin DE, Fried J, Toscano K, Leeuwenburgh C, et al. Autophagy in the heart and liver during normal aging and calorie restriction. *Rejuvenation Res* 2007;10:281–92.
- [37] Nakai A, Yamaguchi O, Takeda T, Higuchi Y, Hikoso S, Taniike M, et al. The role of autophagy in cardiomyocytes in the basal state and in response to hemodynamic stress. *Nat Med* 2007;13:619–24.
- [38] Terman A, Brunk UT. Autophagy in cardiac myocyte homeostasis, aging, and pathology. *Cardiovasc Res* 2005;68:355–65.
- [39] Gottlieb RA, Carreira RS. Autophagy in health and disease. 5. Mitophagy as a way of life. *Am J Physiol Cell Physiol* 2010;299:C203–10.
- [40] McMullen JR, Sherwood MC, Tarnavski O, Zhang L, Dorfman AL, Shioi T, et al. Inhibition of mTOR signaling with rapamycin regresses established cardiac hypertrophy induced by pressure overload. *Circulation* 2004;109:3050–5.
- [41] Harrison DE, Strong R, Sharp ZD, Nelson JF, Astle CM, Flurkey K, et al. Rapamycin fed late in life extends lifespan in genetically heterogeneous mice. *Nature* 2009;460:392–5.
- [42] van der Meer RW, Rijzewijk LJ, Diamant M, Hammer S, Schar M, Bax JJ, et al. The ageing male heart: myocardial triglyceride content as independent predictor of diastolic function. *Eur Heart J* 2008;29:1516–22.
- [43] Rijzewijk LJ, van der Meer RW, Smit JW, Diamant M, Bax JJ, Hammer S, et al. Myocardial steatosis is an independent predictor of diastolic dysfunction in type 2 diabetes mellitus. *J Am Coll Cardiol* 2008;52:1793–9.



SHORT REPORT

Simple autogeneic feeder cell preparation for pluripotent stem cells

Weizhen Li^{a,1}, Hiromi Yamashita^{a,1}, Fumiyuki Hattori^{a,b,*}, Hao Chen^a, Shugo Tohyama^a, Yusuke Satoh^{a,c}, Erika Sasaki^d, Shinsuke Yuasa^a, Shinji Makino^a, Motoaki Sano^a, Keiichi Fukuda^{a,*}

^a Division of Cardiology, Department of Medicine, Keio University School of Medicine, 35 Shinanomachi, Shinjuku-ku, Tokyo 160-8582, Japan

^b Asubio Pharma Co., Ltd. 6-4-3, Minatojimaminami-cho, Chuo-ku, Kobe-city, Hyogo 650-0047, Japan

^c Division of Basic Biological Sciences, Keio University Faculty of Pharmacy, 1-5-30 Shibakoen, Minato-ku, Tokyo 105-8512, Japan

^d Department of Applied Developmental Biology, Central Institute for Experimental Animals, 1430 Nogawa, Miyamae-ku, Kawasaki, Kanagawa 216-0001, Japan

Received 17 July 2010; received in revised form 21 September 2010; accepted 21 September 2010

Abstract Mouse embryonic fibroblasts (MEFs) are the most commonly used feeder cells for pluripotent stem cells. However, autogeneic feeder (AF) cells have several advantages such as no xenogeneic risks and reduced costs. In this report, we demonstrate that common marmoset embryonic stem (cmES) cells can be maintained on common marmoset AF (cmAF) cells. These cmES cells were maintained on cmAF cells for 6 months, retaining their morphology, normal karyotype, and expression patterns for the pluripotent markers Oct-3/4, Nanog, SSEA-3, SSEA-4, TRA-1-60, and TRA-1-81, as well as their ability to differentiate into cardiac and neural cells. Antibody array analysis revealed equivalent protein expression profiles between cmES cells maintained on cmAF cells and MEFs. In addition, similarly prepared human embryonic stem (hES) and induced pluripotent stem (hiPS) cell-derived AF cells supported the growth of and maintained the morphology and pluripotent marker expressions of hES and hiPS cells, respectively. DNA microarray analysis revealed that these hES and hiPS cells had mRNA expression profiles similar to those of hES and hiPS cells maintained on MEFs, respectively. Taken together, these findings imply that AF cells can replace MEFs in the routine maintenance of primate pluripotent stem cells.

© 2010 Elsevier B.V. All rights reserved.

Introduction

Since human embryonic stem (hES) cells were first established by Thomson et al. in 1998, promising results have been obtained with these cells (Thomson et al., 1998). However, owing to ethical problems and concerns about clinical safety, hES cells have not yet been used in clinical studies. Nonhuman primates and their ES and induced pluripotent stem (iPS) cells are expected to be effective preclinical models given their close genetic relationships to humans, as compared with

* Corresponding authors. F. Hattori is to be contacted at Division of Cardiology, Department of Medicine, Keio University School of Medicine, 35 Shinanomachi, Shinjuku-ku, Tokyo 160-8582, Japan. Fax: +81 3 5363 3875. K. Fukuda, fax: +81 3 5363 3875.

E-mail addresses: hattori.fumiyuki.ef@asubio.co.jp (F. Hattori), kfukuda@sc.itc.keio.ac.jp (K. Fukuda).

¹ Weizhen Li and Hiromi Yamashita equally contributed to this study.

rodents (Hearn, 2001; Nakatsuji and Suemori, 2002). Sasaki and co-workers recently established common marmoset ES (cmES) and iPS cell lines, and green fluorescent protein (GFP)-transgenic marmosets (Sasaki et al., 2005; Sasaki et al., 2009; Tomioka et al., 2010), and described the efficient differentiation of neural cells from cmES cells (Sasaki et al., 2005). Chen et al. also reported successful differentiation of cardiomyocytes from cmES cells and described their characterization (Chen et al., 2008).

Recently, iPS cells have been established in rodents (Takahashi and Yamanaka, 2006), nonhuman primates (Tomioka et al., 2010; Wu et al., 2010; Liu et al., 2008), and humans (Takahashi et al., 2007). Clinical applications for these cells are also eagerly awaited, since iPS cells with a genetic background identical to that of the patient can be generated with less ethical concerns. Even though several improvements have been made to combat initial problems, clinical application of human iPS (hiPS) cells is still controversial due to a number of safety concerns.

Common technical constraints for the therapeutic application of hES and hiPS cells also remain. One such limitation is avoiding the use of xenogeneic materials, since there is a risk of cross-transfer of potential pathogens and unexpected genes. To date, various xenogeneic factor-free culture methods have been developed to replace the MEFs used for culturing hES cells, such as immortalized MEFs (Choo et al., 2006), Matrigel (Xu et al., 2001; Akopian et al., 2010), mixed extracellular matrix (Amit and Itskovitz-Eldor, 2006), human-derived primary (Cheng et al., 2003; Lee et al., 2005) and immortalized feeder cells (Unger et al., 2009), suspension culture systems (Steiner et al., 2010; Singh et al., 2010; Olmer et al., 2010; Amit et al., 2010), and autogeneic feeder (AF) cells (Amit and Itskovitz-Eldor, 2006; Choo et al., 2008; Stojkovic et al., 2005; Wang et al., 2005), as well as several xenogeneic factor-free media (Akopian et al., 2010) which can be combined with xeno-free feeders and feeder-free methods. Nevertheless as shown in the report from the International Stem Cell Initiative, most xenogeneic factor-free culture systems based on feeder-free conditions are biased toward hES cell lines (Akopian et al., 2010), suggesting that the MEF feeder system remains the standard because it ensures stable and reliable maintenance for every pluripotent stem cell line. Also in our hands, the MEF feeder system is still the most reliable and general method for maintaining cmES and hES cells, and hiPS cells. Therefore, it is necessary to develop further options for alternative human feeder cells.

AF systems for hES cells have been reported by two groups; the first group derived AF cells via embryoid body (EB) formation (Stojkovic et al., 2005), while the second group generated a stable cell line from differentiated hES cells (Choo et al., 2008). In the present report, we describe a novel method for the preparation of AF cells derived from spontaneously differentiated cells for use in the routine maintenance of pluripotent stem cells. In addition, we report a common method for the preparation of AF cells for different nonhuman primate and human pluripotent stem cells.

Results

Under our routine experimental conditions, cmES, hES, and hiPS cells stably self-renew on MEFs. However a small fraction of each colony contains spontaneously differentiat-

ed cells that have sprouted from the edges of the colonies. During routine passaging, we found that the weak trypsin and collagenase treatment detached preferentially the undifferentiated cells of the colonies, leaving the differentiated cells attached to the plate (Fig. 1a). Since the detached cells had features typical of fibroblasts, we expected that they could be used as AF cells. Previously, these cells would have been discarded, so we term our AF preparation the "cell recycling system." The principle underlying this phenomenon is shown in Fig. 1b.

We cultured the residual cells for 2–4 weeks until they reached subconfluence. The cultivation period to the first passage varied depending on the initial concentration of differentiated cells. The period of time between the passages was approximately 3–5 days. Between the first and third passages, we estimated that the cells had a doubling time of about 20 h. To investigate the relationship between passage number and ability to maintain the undifferentiated state of the cmES cells, we seeded cmES cell clumps onto mitomycin C-treated cmAF cells of various passage numbers, and observed the morphology of the cells under the microscope (Fig. 1c). We found that the cmAF cells that underwent up to three passages maintained the cmES cells without any obvious morphologic alteration of the cmES cells (Fig. 1c). In contrast, when we used cmAF cells after the fourth passage, we found a significant decrease in their maintenance capability. Therefore, we used cmAF cells at the third passage for routine culturing of cmES cells. cmAF cells that were freshly treated with mitomycin C could maintain cmES cells for 1 week; thereafter, they showed decreased viability and maintenance ability. To investigate whether residual MEFs were diluted during cmAF expansion, we performed immunohistochemical analysis for human nuclear antigen (Chen et al., 2008) on cultures of cmAF cells. We found no human nuclear antigen-negative cells (residual MEFs) by fluorescent microscopy (Fig. 1d), which meant that the MEFs had been eliminated during the three passages. The mitomycin C-treated and untreated cmAF cells were successfully stored in the long-term using slow-freezing methods. The viability of the recovered cmAF cells was typically 80 to 90%.

We prepared consecutive batches of cmAF cells from cmES cells that had been cultured on cmAF cells, and maintained the cmES cells in this system for more than 6 months. The cmES cells cultured on cmAF cells for 6 months expressed Oct-3/4, Nanog, SSEA-3, SSEA-4, TRA-1-60, and TRA-1-81 (Fig. 2a). We also confirmed that the cmES cells possessed alkaline phosphatase activity, which is a typical feature of pluripotent stem cells (Fig. 2a). Cytogenetic analysis of the cmES cells that were long-term-cultured on cmAF cells revealed that they retained the normal karyotype of 46XX (Fig. 2b).

To investigate the differentiation ability of the cmES cells cultured on cmAF cells, we induced cardiogenic and neurogenic differentiation. The cmES cells differentiated into cardiomyocytes via embryoid body formation (Fig. 3a). We partially dispersed the EBs and attached them to fibronectin-coated dishes. Immunohistochemical analysis revealed that the EBs expressed Nkx2.5 and sarcomeric α -actinin, indicating that they were cardiomyocytes (Fig. 3b, left panel). We induced neurogenic differentiation by serum withdrawal and retinoic acid stimulation. Thus, we observed sprouting filamentous cells from the attached core of the EBs (Fig. 3b, right panel). We demonstrated immunofluorescence staining for β III tubulin,

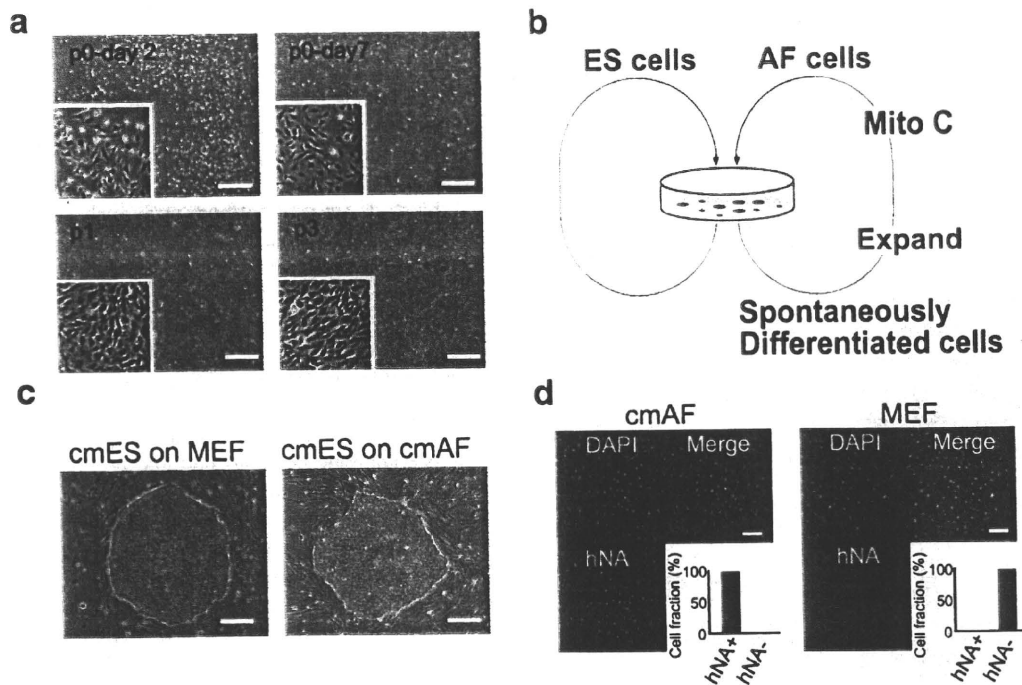


Figure 1 Preparation and application of cmAF cells to cmES cell culturing. (a) Spontaneously differentiated cells that remain on the culture dish are expanded. (b) Schematic representation of the preparation of cmAF cells and the culturing of cmES cells. (c) Morphology of cmES cells cultured on either MEFs (left) or cmAF cells (right). (d) Absence of MEF contamination in the cmAF cells (p3). The right panel shows MEFs used as a negative control in the immunohistochemical detection of human nuclear antigen (hNA). Scale bars: (a and c) 500 μm ; (d) 200 μm .

which is a marker for mature neurons, and confirmed that some of the cells expressed β III tubulin.

Furthermore, to demonstrate the similarity of cmAF cells and MEFs, we analyzed the protein expression profiles of cmES cells cultured on cmAF cells and MEFs, taking advantage of antibody (protein) arrays that are applicable to a broad range of species from rodents to humans. We used the Panorama antibody microarray XP725 kit, which consists of 725 antibodies that have been validated by the manufacturer for studies of mouse and human samples. These antibodies represent families of proteins known to be involved in a variety of important biological pathways, including cell signaling, matrix processing, cell growth, and apoptosis. We analyzed Cy3 labeling of the total protein extracts from cmES cells cultured on cmAF cells or MEFs. Each Cy3-labeled protein was bound to an individual antibody-arrayed glass slide. The fluorescent signals were evaluated using a scanner (Fig. 3c, left). Few proteins had greater than twofold expression changes between cmES cells cultured on cmAF cells and MEFs, indicating that cmES cells cultured on cmAF cells and MEFs have similar protein expression profiles (Fig. 3c, right). We also compared cmES cells cultured on cmAF cells with purified common marmoset ES cell-derived cardiomyocytes as a control experiment. Several differences in protein expression were observed between the cmES cells and purified cardiomyocytes; these included proteins reported to be expressed in cardiomyocytes, such as histone deacetylase 2 (Lu and Yang, 2009), estrogen receptor, and in pluripotent stem cells, such as mitogen and stress activated kinase (Arthur and Cohen, 2000), C-src tyrosine kinase, and Coffilin (Fig. 3d).

Next, we applied our feeder preparation method to hES and hiPS cells (Fig. 4). The hAF and hiAF cells prepared from hES and

hiPS cells were found to maintain hES and hiPS cells for more than 2 months, respectively (Fig. 4a). To investigate whether the MEFs were diluted during the expansion of hiAF cells, we performed immunofluorescent staining for human nuclear antigens with analysis by FACS. Almost all the prepared hiAF cells were positive for human nuclear antigen (Fig. 4b). To further investigate whether the MEFs were diluted during the expansion of hAF cells, we used a stably GFP-expressing hES cell line for hAF cell preparation. We randomly observed five visual fields under the microscope. As a result, no GFP-negative cells (MEFs) were found in the prepared hAF cells (Supplementary Fig. 2). Taken together, these findings show that residual MEFs are eliminated in hiAF cells. Next, we investigated the pluripotency of hiPS cells maintained on hiAF cells by immunofluorescent stainings including microscopic observation (Supplementary Fig. 3) and FACS analysis of SSEA-4, TRA-1-81, Nanog, and Oct-3/4, and confirmed that almost all the hiPS cells expressed the four pluripotent markers (Fig. 4c). We also performed DNA expression array analysis of the hES and hiPS cells that were maintained long-term on hAF and hiAF cells, respectively. Equivalent mRNA expression levels of the pluripotency-related genes including *oct-3/4*, *nanog*, *sox-2*, *lin28*, and *c-myc* were observed. Global gene expression profiles were also quite similar in both cases (Fig. 4d, left). In contrast, two comparative expression profiles between hES and hiPS cells and their differentiating EBs indicated the marked existence of differentially expressed genes (Fig. 4d, right). In addition, a similar magnitude of difference to the results shown in the left panel of Fig. 4d was seen when comparing global gene expression profiles for hES and hiPS cells during different passage numbers (Supplementary Fig. 4). All these results show

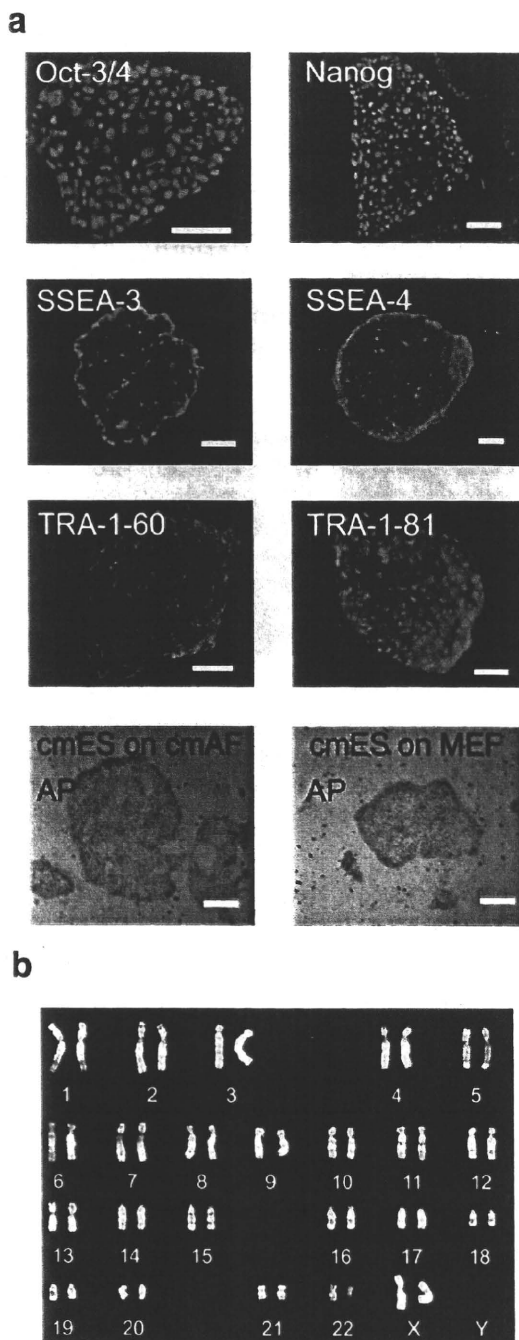


Figure 2 Pluripotent marker expression and cytogenetic analyses of cmES cells cultured on cmAF cells. (a) Immunofluorescence staining for Oct-3/4, Nanog, SSEA-3, SSEA-4, TRA-1-30, and TRA-1-80 of cmES cells cultured on cmAF cells for 6 months. Alkaline phosphatase activities of cmES cells cultured on either cmAF cells (left panel) or MEFs (right panel). (b) Cytogenetic analysis of cmES cells cultured on cmAF cells for 6 months. Scale bar: (a) 300 μ m.

that our hAF and hiAF cells can maintain hES cells in an undifferentiated state and in a condition quite similar to that achieved with MEFs.

Discussion

We have demonstrated the preparation of AF cells from three different cell sources using a common method. These AF cells succeeded in effectively maintaining their pluripotent stem cells.

In this study, we used antibody array analyses to characterize cmES cells. Quite similar protein expression profiles were observed between cmES cells cultured on cmAF cells and MEFs. However, in contrast, various differentially expressed proteins were observed in purified cmES cell-derived cardiomyocytes compared to cmES cells. These results validate the usefulness of this system, and indicate a similar efficacy of cmAF cells compared to MEFs for the maintenance of cmES cells. The mRNA expression profiles produced by global gene array analyses comparing hES cells cultured on hAF cells and MEFs and hiPS cells cultured on hiAF cells and MEFs revealed an overall high similarity in profiles; however, they were not perfectly identical. The differential gene expression profiles comparing different passage numbers of the same human pluripotent stem cells maintained with the same feeder cells showed a similar dispersion to those observed between human pluripotent stem cells maintained with MEF and AF cells. These results suggest that some allowable gene expression changes might spontaneously occur during long-term culture in pluripotent stem cells, although the genes related with pluripotency must be maintained.

Using our routine preparation of cmAF cells, approximately 1×10^8 cells can be obtained from a single 10-cm dish and three cell passages. This number of cmAF cells is sufficient to prepare 100 10-cm dishes for cmES cell culturing. In contrast, 1×10^7 MEFs are typically obtained from a single mouse embryo under our experimental conditions. Thus we believe that our AF system has a comparable cell yield to that of the MEF system.

As potential therapies using personalized iPS cells become possible, it may be reasonable to maintain an individual's hiPS cell line using their AF cells, because there would be no concerns of transfer of allogenic antigens or infectious viruses from the feeder cells. Even in the case of mass production of therapeutic cells from banked pluripotent stem cells, techniques have not yet been established for maintaining pluripotent stem cells under xenogeneic factor-free conditions at a reasonable cost.

Conclusions

The present study establishes an effective method for preparing AF cells which is applicable to cmES, hES, and hiPS cells. We believe that the results of the present study pave the way for the reliable and economic production of alternative feeder cells for pluripotent stem cells.

Materials and methods

Maintenance of undifferentiated cmES, hES cells, and hiPS cells

The cmES cells (cell line No. 20; Central Institute of Experimental Animals, Kawasaki, Japan), hES cells (khES-2; Institute for Integrated Cell-Material Sciences, Kyoto University), and hiPS cells (G4; Center for iPS Cell Research and

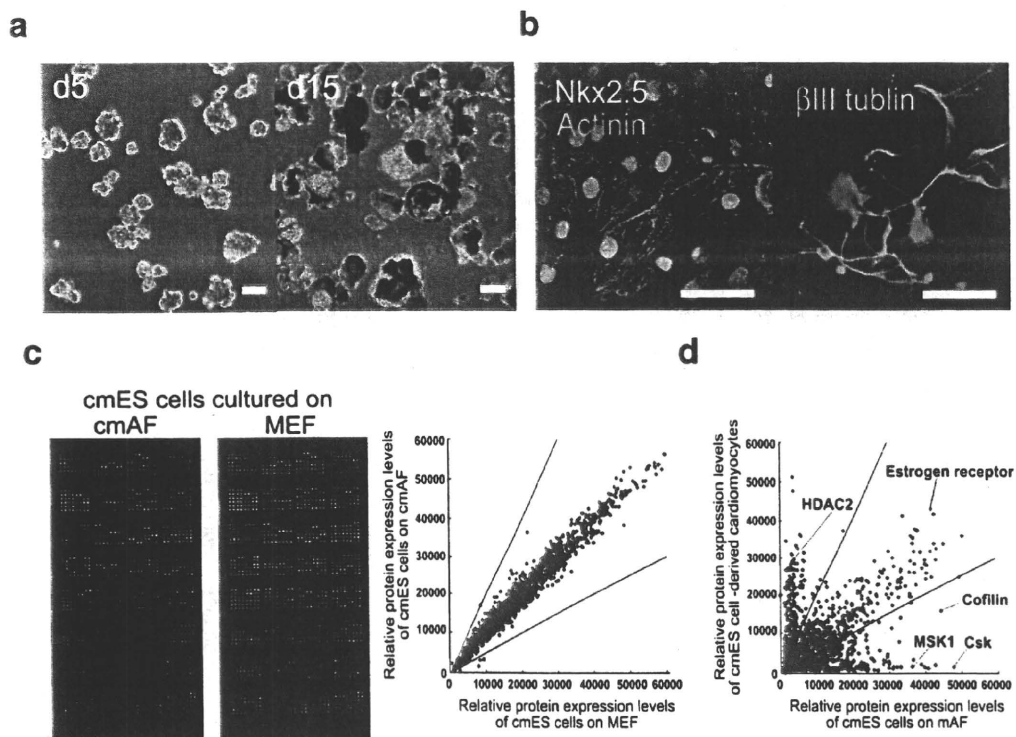


Figure 3 *In vitro* differentiation abilities of the cultured cmES cells and antibody array analysis of cmES cells cultured on either cmAF cells or MEFs. (a) EB formation of cmES cells during long-term culturing on cmAF cells. (b) Cardiomyocytes and neurons differentiate from cmES cells during long-term culturing on cmAF cells. (c) Antibody array analysis was performed on Cy3-labeled total protein extracts from cmES cells cultured on either cmAF cells or MEFs for 50 days. The left panels show the raw images of the Cy3 signals. The scatter plot shows the relative fluorescence levels for the antibodies used to stain cmES cells cultured on cmAF cells (*y*-axis) and MEFs (*x*-axis). (d) Antibody array analysis was performed on protein extracts from cmES cells cultured on cmAF cells and purified cmES cell-derived cardiomyocytes. The scatter plot shows the relative fluorescence levels for the antibodies used to stain purified cmES cell-derived cardiomyocytes (*y*-axis) and cmES cells cultured on cmAF cells (*x*-axis). Twofold differences, representing the threshold in this experiment, are indicated as lines in the plots (c, d). Scale bars: (a) 300 μ m; (b) 100 μ m.

Application, Institute for Integrated Cell-Material Sciences, Kyoto University) were maintained as described previously (Chen et al., 2008; Hattori et al., 2010). Briefly, cmES cells were maintained on feeder cells in cmES cell medium, which consisted of 80% Knockout Dulbecco's modified Eagle's medium (KO-DMEM; Invitrogen, Carlsbad, CA, USA), 20% Knockout Serum Replacement (KSR; Invitrogen), 0.1 mM nonessential amino acids (Sigma Chemical Company), 2 mM L-glutamine (Sigma, St. Louis, MO), 0.1 mM β -mercaptoethanol (Sigma), and 4 ng/mL basic fibroblast growth factor (Wako Pure Chemical Industries, Osaka, Japan). hES and hiPS cells were similarly maintained, except that Dulbecco's modified Eagle's medium/Nutrient Mixture F-12 Ham's (1/1 ratio, DMEM-F12; Sigma) was used instead of KO-DMEM. The cmES and hES cells were passaged every 5–7 days. Typically, we cultured pluripotent stem cells in 15-cm dishes (Becton–Dickinson, NJ, USA). Using this method, all reagent amounts were suitable for 15-cm dish cultures.

Passage of pluripotent stem cells

All cmES, hES, and hiPS cells were treated with 2 mL of 0.25% trypsin (Becton–Dickinson), 0.1% collagenase type 3 (Worthington Biochemical Corp., NJ, USA), 20% KSR, and 1 mM CaCl_2 in phosphate-buffered saline at 37 $^{\circ}$ C for 5–15 min, which resulted

in disruption of the boundaries between the pluripotent stem cells and the feeder cells. Then, 5 mL of DMEM supplemented with 10% fetal bovine serum (FBS; Biowest, FL, USA) was added and the cells were gently pipetted several times, which detached all the pluripotent stem cell colonies and most of the feeder cells from the dish. The cells were separated into three fractions by size, <40 μ m, between 40 and 100 μ m, and >100 μ m, using cell strainers with mesh pore diameters of 40 and 100 μ m (Becton–Dickinson). These procedures are illustrated in Supplementary Fig. 1a. This process eliminated feeder cells (Supplementary Fig. 1b). The collected pluripotent stem cell colonies of the correct size (larger than 40 μ m and smaller than 100 μ m) were seeded onto a new plate with feeder cells.

Preparation of AF cells

A low number of differentiating cells remained on the culture dish after passage (Fig. 1a). These cells were the seeds of the AF cells, and they were propagated in DMEM (Wako) supplemented with 10% FBS. Typically, propagation to near confluence took 10–15 days for cmAF cells and 20–30 days for human AF (hAF) and iAF (hiAF) cells. For passaging, the cells were detached and dispersed by treatment with 0.25% trypsin-EDTA solution (TE; Invitrogen) at 37 $^{\circ}$ C for 10 min. A cell

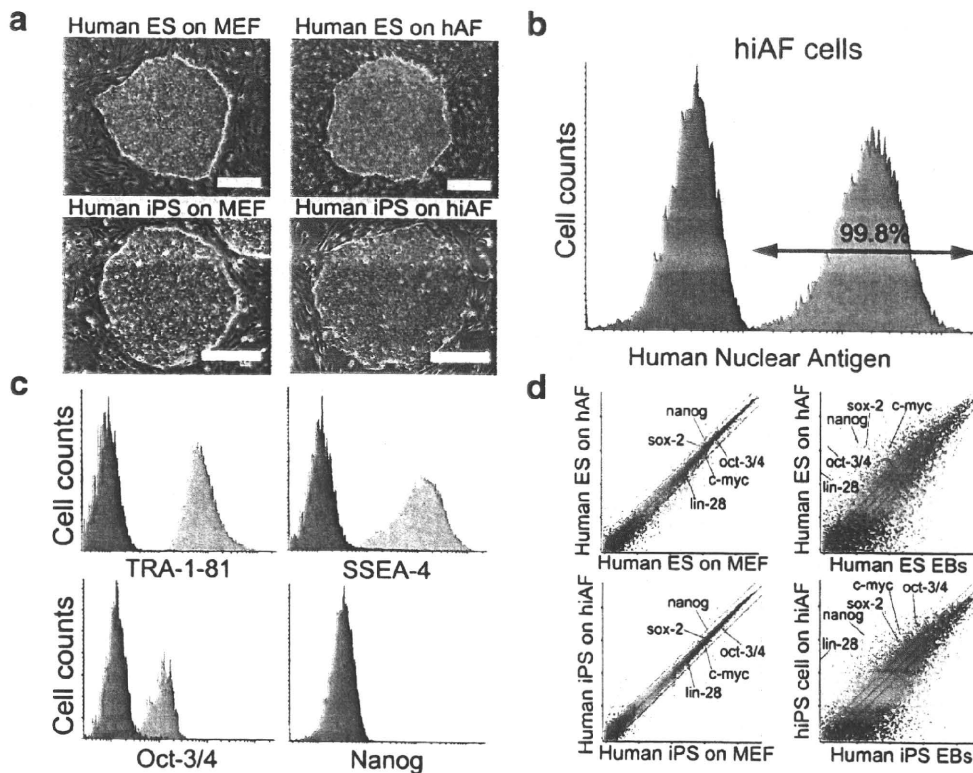


Figure 4 Application of hAF and hiAF cells to the cultivation of hES and hiPS cells, and DNA microarray analysis. (a) Morphology of hES (upper panels) and hiPS (lower panels) cells cultured on either MEFs (left panels) or hAF and hiAF cells (right panels). (b) Human nuclear antigen was immunofluorescently detected and analyzed by FACS (red histogram) in the hiAF cells. The negative control (second antibody only) is shown as the blue histogram. (c) Human iPS cells which were maintained long term by hiAF cells were passaged, as described under Materials and methods, enzymatically dispersed, immunofluorescently stained for TRA-1-81, SSEA-4, Oct-3/4, and Nanog, and then analyzed by FACS. The negative control (second antibody only) is shown as the blue histogram. (d) DNA microarray analysis of mRNA extracted from hES (upper left panel) and hiPS (lower left panel) cells that were cultured on either hAF and hiAF cells (y-axis) or MEFs (x-axis) for 32 or 35 days, respectively. Similarly, comparisons between hES cells grown on hAF cells (upper) or hiPS cells grown on hiAF cells (lower) and their EBs are shown in the right panels. The scatter plot shows the relative expression level (threshold:10) for each gene. Twofold differences are indicated as lines in the plot. Scale bars: (a) 300 μm .

strainer with mesh pore diameter of 40 μm (Becton-Dickinson) was used to eliminate the residual large cell clumps (diameter >40 μm). The purified AF cells were plated onto new 0.1% gelatin-coated dishes that contained DMEM supplemented with 10% FBS. For all the cmES, hES, and hiPS cells, confluence was achieved in 3–5 days, and these cells were subsequently passaged to the next generation using a 5-times dilution. The second or third generation of AF cells were treated with 10 $\mu\text{g}/\text{mL}$ of mitomycin C at 37 $^{\circ}\text{C}$ for 3 h, and cryopreserved at -150 $^{\circ}\text{C}$ in Cellbanker solution (Mitsubishi Chemical, Tokyo, Japan). The cmAF, hAF, or hiAF cells recovered from the cryostocks were seeded onto 0.1% gelatin-coated dishes at a concentration of 2×10^6 cells per 15-cm dish.

Supplementary materials related to this article can be found online at doi:10.1016/j.scr.2010.09.003.

Acknowledgments

This study was supported in part by research grants from the Special Coordination Funds for Promoting Science and Technology in the Japanese Ministry of Education, Culture,

Sports, Science, and Technology and from the Japan-China Medical Association. This work was also in part supported by KAKENHI and New Energy and Industrial Technology Development Organization (NEDO).

References

- Akopian, V., Andrews, P.W., Beil, S., Benvenisty, N., Brehm, J., Christie, M., Ford, A., Fox, V., Gokhale, P.J., Healy, L., Holm, F., Hovatta, O., Knowles, B.B., Ludwig, T.E., McKay, R.D., Miyazaki, T., Nakatsuji, N., Oh, S.K., Pera, M.F., Rossant, J., Stacey, G.N., Suemori, H., 2010. Comparison of defined culture systems for feeder cell free propagation of human embryonic stem cells. *In Vitro Cell. Dev. Biol. Anim.* 46, 247–258.
- Amit, M., Itskovitz-Eldor, J., 2006. Feeder-free culture of human embryonic stem cells. *Methods Enzymol.* 420, 37–49.
- Amit, M., Chebath, J., Margulets, V., Laevsky, I., Miropolsky, Y., Shariki, K., Peri, M., Blais, I., Slutsky, G., Revel, M., Itskovitz-Eldor, J., 2010. Suspension culture of undifferentiated human embryonic and induced pluripotent stem cells. *Stem Cell Rev.* 6, 248–259.
- Arthur, J.S., Cohen, P., 2000. MSK1 is required for CREB phosphorylation in response to mitogens in mouse embryonic stem cells. *FEBS Lett.* 482, 44–48.

- Chen, H., Hattori, F., Murata, M., Li, W., Yuasa, S., Onizuka, T., Shimoji, K., Ohno, Y., Sasaki, E., Kimura, K., Hakuno, D., Sano, M., Makino, S., Ogawa, S., Fukuda, K., 2008. Common marmoset embryonic stem cell can differentiate into cardiomyocytes. *Biochem. Biophys. Res. Commun.* 369, 801–806.
- Cheng, L., Hammond, H., Ye, Z., Zhan, X., Dravid, G., 2003. Human adult marrow cells support prolonged expansion of human embryonic stem cells in culture. *Stem Cells* 21, 131–142.
- Choo, A., Padmanabhan, J., Chin, A., Fong, W.J., Oh, S.K., 2006. Immortalized feeders for the scale-up of human embryonic stem cells in feeder and feeder-free conditions. *J. Biotechnol.* 122, 130–141.
- Choo, A., Ngo, A.S., Ding, V., Oh, S., Kiang, L.S., 2008. Autogeneic feeders for the culture of undifferentiated human embryonic stem cells in feeder and feeder-free conditions. *Methods Cell Biol.* 86, 15–28.
- Hattori, F., Chen, H., Yamashita, H., Tohyama, S., Satoh, Y.S., Yuasa, S., Li, W., Yamakawa, H., Tanaka, T., Onitsuka, T., Shimoji, K., Ohno, Y., Egashira, T., Kaneda, R., Murata, M., Hidaka, K., Morisaki, T., Sasaki, E., Suzuki, T., Sano, M., Makino, S., Oikawa, S., Fukuda, K., 2010. Nongenetic method for purifying stem cell-derived cardiomyocytes. *Nat. Methods* 7, 61–66.
- Hearn, J.P., 2001. Embryo implantation and embryonic stem cell development in primates. *Reprod. Fertil. Dev.* 13, 517–522.
- Lee, J.B., Lee, J.E., Park, J.H., Kim, S.J., Kim, M.K., Roh, S.I., Yoon, H.S., 2005. Establishment and maintenance of human embryonic stem cell lines on human feeder cells derived from uterine endometrium under serum-free condition. *Biol. Reprod.* 72, 42–49.
- Liu, H., Zhu, F., Yong, J., Zhang, P., Hou, P., Li, H., Jiang, W., Cai, J., Liu, M., Cui, K., Qu, X., Xiang, T., Lu, D., Chi, X., Gao, G., Ji, W., Ding, M., Deng, H., 2008. Generation of induced pluripotent stem cells from adult rhesus monkey fibroblasts. *Cell Stem Cell* 3, 587–590.
- Lu, Y., Yang, S., 2009. Angiotensin II induces cardiomyocyte hypertrophy probably through histone deacetylases. *Tohoku J. Exp. Med.* 219, 17–23.
- Nakatsuji, N., Suemori, H., 2002. Embryonic stem cell lines of nonhuman primates. *ScientificWorldJournal* 2, 1762–1773.
- Olmer, R., Haase, A., Merkert, S., Cui, W., Palecek, J., Ran, C., Kirschning, A., Scheper, T., Glage, S., Miller, K., Curnow, E.C., Hayes, E.S., Martin, U., 2010. Long term expansion of undifferentiated human iPS and ES cells in suspension culture using a defined medium. *Stem Cell Res.* 5, 51–64.
- Sasaki, E., Hanazawa, K., Kurita, R., Akatsuka, A., Yoshizaki, T., Ishii, H., Tanioka, Y., Ohnishi, Y., Suemizu, H., Sugawara, A., Tamaoki, N., Izawa, K., Nakazaki, Y., Hamada, H., Suemori, H., Asano, S., Nakatsuji, N., Okano, H., Tani, K., 2005. Establishment of novel embryonic stem cell lines derived from the common marmoset (*Callithrix jacchus*). *Stem Cells* 23, 1304–1313.
- Sasaki, E., Suemizu, H., Shimada, A., Hanazawa, K., Oiwa, R., Kamioka, M., Tomioka, I., Sotomaru, Y., Hirakawa, R., Eto, T., Shiozawa, S., Maeda, T., Ito, M., Ito, R., Kito, C., Yagihashi, C., Kawai, K., Miyoshi, H., Tanioka, Y., Tamaoki, N., Habu, S., Okano, H., Nomura, T., 2009. Generation of transgenic non-human primates with germline transmission. *Nature* 459, 523–527.
- Singh, H., Mok, P., Balakrishnan, T., Rahmat, S.N., Zweigerdt, R., 2010. Up-scaling single cell-inoculated suspension culture of human embryonic stem cells. *Stem Cell Res.* 4, 165–179.
- Steiner, D., Khaner, H., Cohen, M., Even-Ram, S., Gil, Y., Itsykson, P., Turetsky, T., Idelson, M., Aizenman, E., Ram, R., Berman-Zaken, Y., Reubinoff, B., 2010. Derivation, propagation and controlled differentiation of human embryonic stem cells in suspension. *Nat. Biotechnol.* 28, 361–364.
- Stojkovic, P., Lako, M., Stewart, R., Przyborski, S., Armstrong, L., Evans, J., Murdoch, A., Strachan, T., Stojkovic, M., 2005. An autogeneic feeder cell system that efficiently supports growth of undifferentiated human embryonic stem cells. *Stem Cells* 23, 306–314.
- Takahashi, K., Yamanaka, S., 2006. Induction of pluripotent stem cells from mouse embryonic and adult fibroblast cultures by defined factors. *Cell* 126, 663–676.
- Takahashi, K., Tanabe, K., Ohnuki, M., Narita, M., Ichisaka, T., Tomoda, K., Yamanaka, S., 2007. Induction of pluripotent stem cells from adult human fibroblasts by defined factors. *Cell* 131, 861–872.
- Thomson, J.A., Itskovitz-Eldor, J., Shapiro, S.S., Waknitz, M.A., Swiergiel, J.J., Marshall, V.S., Jones, J.M., 1998. Embryonic stem cell lines derived from human blastocysts. *Science* 282, 1145–1147.
- Tomioka, I., Maeda, T., Shimada, H., Kawai, K., Okada, Y., Igarashi, H., Oiwa, R., Iwasaki, T., Aoki, M., Kimura, T., Shiozawa, S., Shinohara, H., Suemizu, H., Sasaki, E., Okano, H., 2010. Generating induced pluripotent stem cells from common marmoset (*Callithrix jacchus*) fetal liver cells using defined factors, including Lin28. *Genes Cells.*
- Unger, C., Gao, S., Cohen, M., Jaconi, M., Bergstrom, R., Holm, F., Galan, A., Sanchez, E., Irion, O., Dubuisson, J.B., Giry-Laterriere, M., Salmon, P., Simon, C., Hovatta, O., Feki, A., 2009. Immortalized human skin fibroblast feeder cells support growth and maintenance of both human embryonic and induced pluripotent stem cells. *Hum. Reprod.* 24, 2567–2581.
- Wang, Q., Fang, Z.F., Jin, F., Lu, Y., Gai, H., Sheng, H.Z., 2005. Derivation and growing human embryonic stem cells on feeders derived from themselves. *Stem Cells* 23, 1221–1227.
- Wu, Y., Zhang, Y., Mishra, A., Tardif, S.D., Hornsby, P.J., 2010. Generation of induced pluripotent stem cells from newborn marmoset skin fibroblasts. *Stem Cell Res.* 4, 180–188.
- Xu, C., Inokuma, M.S., Denham, J., Golds, K., Kundu, P., Gold, J.D., Carpenter, M.K., 2001. Feeder-free growth of undifferentiated human embryonic stem cells. *Nat. Biotechnol.* 19, 971–974.

G-CSF influences mouse skeletal muscle development and regeneration by stimulating myoblast proliferation

Mie Hara,¹ Shinsuke Yuasa,^{1,2} Kenichiro Shimoji,¹ Takeshi Onizuka,¹ Nozomi Hayashiji,¹ Yohei Ohno,¹ Takahide Arai,¹ Fumiyuki Hattori,¹ Ruri Kaneda,¹ Kensuke Kimura,¹ Shinji Makino,^{1,2} Motoaki Sano,¹ and Keiichi Fukuda¹

¹Department of Cardiology and ²Center for Integrated Medical Research, Keio University School of Medicine, Shinjuku, Tokyo 160-8582, Japan

After skeletal muscle injury, neutrophils, monocytes, and macrophages infiltrate the damaged area; this is followed by rapid proliferation of myoblasts derived from muscle stem cells (also called satellite cells). Although it is known that inflammation triggers skeletal muscle regeneration, the underlying molecular mechanisms remain incompletely understood. In this study, we show that granulocyte colony-stimulating factor (G-CSF) receptor (G-CSFR) is expressed in developing somites. G-CSFR and G-CSF were expressed in myoblasts of mouse embryos during the midgestational stage but not in mature myocytes. Furthermore, G-CSFR was specifically but transiently expressed in regenerating myocytes present in injured adult mouse skeletal muscle. Neutralization of endogenous G-CSF with a blocking antibody impaired the regeneration process, whereas exogenous G-CSF supported muscle regeneration by promoting the proliferation of regenerating myoblasts. Furthermore, muscle regeneration was markedly impaired in G-CSFR-knockout mice. These findings indicate that G-CSF is crucial for skeletal myocyte development and regeneration and demonstrate the importance of inflammation-mediated induction of muscle regeneration.

Adult skeletal muscle has resident stem cells, called satellite cells, which are responsible for generating new muscle under both physiological and pathophysiologic conditions. Although these muscles have the capacity to regenerate, this capacity has some limitations (Le Grand and Rudnicki, 2007). There are several skeletal muscle diseases such as skeletal muscle dystrophy, myopathy, severe injury, and disuse syndrome for which there are no effective treatments (Shi and Garry, 2006). Although several studies have identified various growth factors and cytokines that regulate skeletal muscle development and regeneration, effective control of regeneration hasn't been achieved using these factors in the clinical setting (Buckingham and Montarras, 2008). Therefore, it is worth elucidating the mechanisms of skeletal muscle regeneration and developing novel regeneration therapies.

After injury to skeletal muscle, neutrophils, monocytes, and macrophages infiltrate the damaged area. Concomitantly, satellite cells differentiate into transient-amplifying myoblasts, which rapidly proliferate, fuse with one another, and regenerate skeletal myotubes. During these processes, inflammation and regeneration are tightly linked. Therefore, it is reasonable to assume that some factors expressed during the inflammatory process influence skeletal muscle regeneration. However, the precise mechanisms remain unknown.

Previously, when we looked for potent differentiation-promoting factors during embryonic stem cell differentiation (Yuasa et al., 2005, 2010), we noted a marked elevation in the expression of G-CSF receptor (G-CSFR; encoded

CORRESPONDENCE

Keiichi Fukuda:
kfukuda@sc.itc.keio.ac.jp

Abbreviations used: APRE, acute phase response element; EGFP, enhanced GFP; ERK, extracellular regulated kinase; G-CSFR, G-CSF receptor; JNK, c-Jun N-terminal kinase; MRF, myogenic regulatory factor.

M. Hara and S. Yuasa contributed equally to this paper.

© 2011 Hara et al. This article is distributed under the terms of an Attribution-Noncommercial-Share Alike-No Mirror Sites license for the first six months after the publication date (see <http://www.rupress.org/terms>). After six months it is available under a Creative Commons License (Attribution-Noncommercial-Share Alike 3.0 Unported license, as described at <http://creativecommons.org/licenses/by-nc-sa/3.0/>).

Supplemental Material can be found at:
<http://jem.rupress.org/content/suppl/2011/03/21/jem.20101059.DC1.html>

715